Advanced Industrial and Engineering Polymer Research 7 (2024) 373–404

Contents lists available at ScienceDirect

Advanced Industrial and Engineering Polymer Research

journal homepage: http://www.keaipublishing.com/aiepr

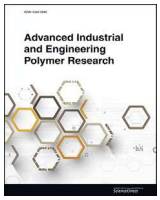

Review Article

Compatibilization of biopolymer blends: A review

Giulia Fredi*, Andrea Dorigato

University of Trento, Department of Industrial Engineering and INSTM Research Unit, Via Sommarive 9, 38123 Trento, Italy

ARTICLE INFO

Article history:
Received 1 September 2023
Received in revised form
9 November 2023
Accepted 9 November 2023

Keywords:
Biopolymers
Blends
Compatibilization
Miscibility
Interface

ABSTRACT

Biopolymers from renewable bio-based resources provide a sustainable alternative to petroleum-derived plastics, but limitations like brittleness and cost restrict applicability. Blending offers an affordable route to combine the advantages of different biopolymers for tailored performance. However, most biopolymer pairs are intrinsically immiscible, necessitating compatibilization to obtain optimal blend morphology, interfacial interaction, and properties. This review summarizes key compatibilization strategies and recent advances in tailoring biopolymer blends. Non-reactive techniques using block or graft copolymers can increase compatibility, though property enhancements are often modest. More impactful are reactive methods, which functionalize and form compatibilizing copolymers in-situ during melt-blending. Nanoparticle incorporation also effectively compatibilizes through interface localization and morphology control. These strategies enable significant toughening and compatibilization of poly(lactic acid) (PLA) and other brittle biopolyesters by blending with ductile polymers such as poly(butylene adipate-*co*-terephthalate)((PBAT) or elastomers like natural rubber. Properly compatibilized PLA blends exhibit major simultaneous improvements in elongation, strength, and impact resistance. Using inexpensive starch decreases cost but requires compatibilization to maintain adequate properties. Nanoparticles additionally impart functionality like barrier and flame retardance. However, quantitatively correlating interaction, processing, morphology, and properties will enable further blend optimization. Developing tailored reactive chemistries and nanoparticles offers potential beyond conventional techniques, and retaining biodegradability is also crucial. Overall, compatibilization facilitates synergistic property combinations from complementary biopolymers, providing eco-friendly, high-performance, and cost-effective alternatives to traditional plastics across diverse applications.

1. Introduction and scope of the work

Bioplastics have been extensively studied in both academic and industrial settings for more than thirty years. The global production of bioplastics has been on a rapid rise, reaching 2.2 million tons (Mt) in 2022 and projected to reach 6.3 Mt by 2027 (Fig. 1(a-b)) [1]. This growth can be attributed to several factors, including heightened environmental awareness, evolving consumer preferences, policy and legislative changes, and advancements in materials and product development. In fact, bioplastics are a promising alternative to conventional plastics, which are often the most efficient, sustainable, and cost-effective choice in the use phase [2] but show margins of improvement in the early stages of their life cycle (i.e., petrochemical origin) as well as in the end-of-life phase (i.e., waste accumulation) [3–6].

In this perspective, bioplastics can effectively respond to both these drawbacks of conventional polymers [6–9]. Biodegradable bioplastics provide alternative waste disposal options, thereby reducing the accumulation of plastic waste in the environment, while bioderived bioplastics contribute to a lower carbon footprint by employing renewable resources [10]. Hence, extensive research has led to the commercialization of many different biopolymers, including poly(lactic acid) (PLA), polyhydroxyalkanoates (PHAs) [11,12], poly(butylene succinate) (PBS) [13], and thermoplastic starch (TPS) [14,15], but also partially biobased poly(ethylene terephthalate) (bioPET) and bio-polyethylene (bioPE), which are similar to their non-renewable counterparts [16,17] (Fig. 1c).

Despite this progress, bioplastics still account for less than 1% of the total global plastics production, which has been 390 Mt in 2022 [18]. It is crucial to increase the market share of bioplastics in order

* Corresponding author.
E-mail addresses: giulia.fredi@unitn.it (G. Fredi), andrea.dorigato@unitn.it (A. Dorigato).

https://doi.org/10.1016/j.aiepr.2023.11.002

List of acronyms and symbols

bioPAs	bio-based polyamides
bioPE	bio-polyethylene
bioPET	biobased poly(ethylene terephthalate)
bioPP	bio-polypropylene
bioPTT	bio-poly(trimethylene terephthalate)
CAB	cellulose acetate butyrate
CNTs	carbon nanotubes
DCP	dicumyl peroxide
DMA	dynamic mechanical thermal analysis
DSC	differential scanning calorimetry
EG	ethylene glycol
E-GMA	ethylene-co-glycidyl methacrylate
ENR	Epoxidized natural rubber
FTIR	Fourier-transform infrared spectroscopy
HV	hydroxyvalerate
HIPS	High-impact polystyrene
LDPE	low-density polyethylene
LLDPE	linear low-density polyethylene
LNR	liquid natural rubber
MA	maleic anhydride
MMT	montmorillonite
MPEG-PLA	poly(ethylene glycol)-polylactide
NMR	nuclear magnetic resonance
NR	natural rubber
OMMT	organomodified montmorillonite
PBA	poly(1,4-butylene adipate)
PBAT	poly(butylene adipate-*co*-terephthalate)
PB-g-SAN	polybutadiene-*graft*-poly(styrene-*co*-acrylonitrile)
PBS	poly(butylene succinate)
PBSA	poly(butylene succinate-*co*-adipate)
PC	polycarbonate
PCL	polycaprolactone
PDLA	poly(D-lactic acid)
PDLLA	poly(D-L-lactic acid)
PEF	poly(ethylene furanoate)
PEG	poly(ethylene glycol)
PEGMA	Glycidyl methacrylate grafted LDPE
PEO	poly(ethylene octene)
PHAs	polyhydroxyalkanoates
PHB	poly(3-hydroxybutyrate)
PHBV	poly(3-hydroxybutyrate-*co*-3-hydroxyvalerate)
PGU	PLA-g-TPU graft copolymers
PLA	poly(lactic acid)
PLLA	poly(L-lactic acid)
PLLCL	poly(L-lactide-*co*-caprolactone)
PMMA	poly(methyl methacrylate)
POE	poly(ethylene octene)
POM	polarized optical microscopy
PPC	poly(propylene carbonate)
PS	polystyrene
PVA or PVOH	polyvinylalcohol
PVPh	poly(vinyl phenol)
ROP	ring-opening polymerization
SAXS	small angle X-ray scattering
SEC	size exclusion chromatography
SEM	Scanning electron microscopy
SME	specific mechanical energy
TEM	Transmission electron microscopy
TGA	thermogravimetric analysis
TPS	thermoplastic starch
TPU	thermoplastic polyurethane
VGN	vinyl functionalized graphene
XRD	X-ray diffraction
ΔG_{mix}	Gibbs free energy of mixing
T_g	Glass transition temperature
Mt	Million tons
χ_{12}	Flory-Huggins interaction parameter
n	degree of polymerization
φ	volume fraction
R	gas constant
T	absolute temperature
δ	Hildebrand solubility parameter
$\Delta\delta_{crit}$	critical solubility parameter difference
ω_a	wetting coefficient
γ	Interfacial energy
γ^d	dispersive component of the surface tension
γ^p	polar component of the surface tension
r	size of the dispersed particles
α	coalescence probability of particles
l	thickness of the interphase
b	effective monomer length
V_r	molar reference volume
η	Viscosity
σ_y	Yield stress
σ_T	Tensile strength
B	Interaction coefficient
n	strain-hardening coefficient
C	stress transfer Coefficient
ΔC_p	specific heat increment
ω	Weight fraction
ΔH^0	Melting enthalpy
W_c	Critical Weber number

to reduce reliance on fossil-based resources, facilitate the transition to a bio-based society, minimize the environmental impact of polymeric materials, and promote a circular economy. However, achieving these objectives requires comprehensive improvements in the mechanical and functional performance of biopolymers, which must be coupled with a substantial reduction in their production cost [19].

These are indeed the two main limitations of biopolymers. Despite the growing production capacity, biopolymers are still expensive when compared to commodity polymers. Additionally, their processability and final mechanical properties are often inferior to those of traditional plastics, or at least fall short of the expectations of converters and users. Consequently, in an attempt to fill the property and cost gap with commodity polymers and meet market demands, biopolymers often require modifications [20].

Among all the approaches to tailor the properties of plastics, one of the most established and cost-effective tools is physical blending, which involves mixing different thermoplastic materials in the molten state. Being less expensive and more straightforward than synthesizing new macromolecules, blending can play a vital role in enhancing the competitiveness of biopolymers. However, as commonly found for standard polymers, the miscibility and compatibility of most biopolymer combinations are not sufficient to provide optimal blend performance, thus necessitating the use of compatibilization techniques.

This paper provides a comprehensive overview of the most recent trends and achievements in the field of biopolymer blends.

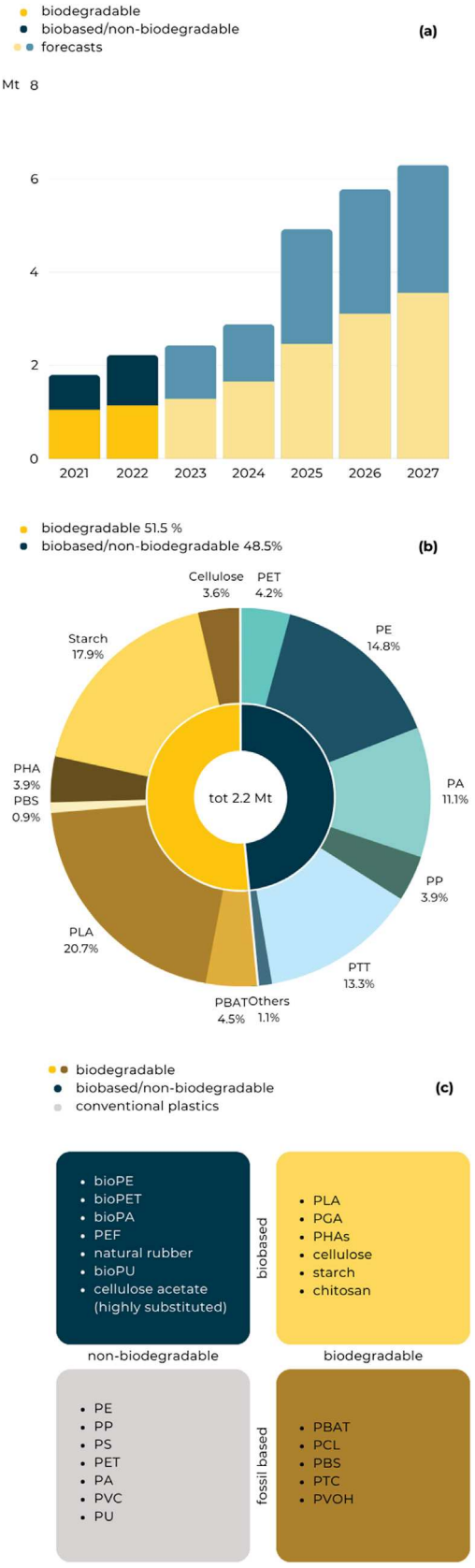

Fig. 1. (a) Global production capacity of bioplastics, data and forecasts (2021–2027); (b) Global production capacity of bioplastics 2022 by material; (c) classification of conventional plastics and bioplastics according to their biodegradability and renewable origin. Data derived from Ref. [1]. Please refer to the acronym list for the definition of the used acronym.

As the most industrially relevant bioplastics are biobased and biodegradable biopolyesters such as PLA, PHAs, or polysaccharides such as starch and cellulose, this review will focus on blends based on these biopolymer classes. More specifically, one of the aims of this review is to highlight the challenges and possibilities provided by biodegradable and compostable blends, as well as the requirements that must be met to comply with the biodegradability standards.

In the next sections, we will first clarify some key concepts about biopolymers and provide the definition of the most important terms, such as “biobased”, “biodegradable”, and “compostable”. Then, after a general introduction on the theory of polymer blends, the most important compatibilization strategies for biopolymers will be reviewed and classified according to the compatibilization technique, with many examples from the recent literature. The subsequent section will describe the characterization methods useful to assess the performance of the applied compatibilization strategy, and the last chapter will illustrate the relationship between blending, compatibilization, and biodegradability.

2. Biopolymers: definitions, properties, and applications

Bioplastics are plastics that are either derived from renewable biomass sources, are capable of biodegrading, or both [1]. The precise definitions of the terms “bio-based” and “biodegradable” when referring to plastics are provided by various international standards [21]. For example, standards such as ISO 17088 and ASTM D6400 lay out specific conditions under which a biodegradable plastic must break down within a certain timeframe in order for it to be considered compostable. The ASTM D6400-19 standard defines the requirements for a product to qualify as compostable in municipal or industrial aerobic composting facilities. According to the standard, the product must degrade during the composting process such that no more than 10% of the original weight remains after sieving through a 2 mm sieve after 84 days in the compost environment. Additionally, 90% of the product's organic carbon content must be converted into carbon dioxide within 180 days. Finally, the standard states that the product must not inhibit the ability of the compost to support plant growth, in comparison to control compost samples prepared without that product. Meeting all three of these criteria is necessary for a product to be considered compostable under the specifications of ASTM D6400-19.

On the other hand, standards including EN 16640 and ASTM 6866 define methods to measure the renewable carbon content in bio-based plastics, regardless of their biodegradability, through techniques such as radiocarbon dating [22]. Based on these definitions, bioplastics can be divided into three main categories (Fig. 1c) [1]: (i) plastics that are both bio-based and biodegradable, such as PLA, PHAs, TPS, and PBS; (ii) plastics that are biodegradable but are made from petrochemical resources rather than biomass, such as poly(butylene adipate-*co*-terephthalate) (PBAT) and polycaprolactone (PCL); and (iii) plastics that are bio-based but not necessarily biodegradable or only partially biodegradable, such as bioPE, bioPET, biopolypropylene (bioPP), and bioderived technical polymers like bio-poly(trimethylene terephthalate) (bioPTT) and some bio-based polyamides (bioPAs).

Among all the applications for bioplastics, packaging accounts for the largest market share by weight, at almost 48% of the total in 2022 (1.1 Mt) [1]. However, bioplastics are also being used in a growing range of other markets, including agriculture, textiles, automotive, and more.

The focus of this review is on bioplastic blends utilizing biodegradable polymers, particularly the major commercially produced biodegradable bioplastics: PLA, starch blends, and PHAs (Fig. 2).

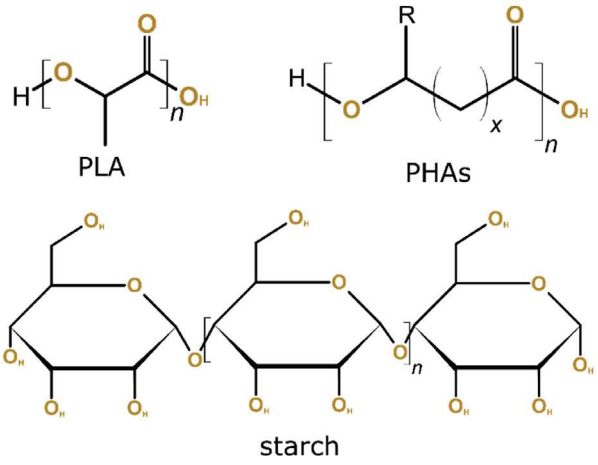

Fig. 2. General formula of PLA, polyhydroxyalkanoates (PHAs) (x = 1 and R=CH_3 for poly(3-hydroxybutyrate) (PHB), while x = 1 and R=C_2H_5 for poly(3-hydroxyvalerate)), and starch (amylose).

2.1. Industrially relevant biobased and biodegradable bioplastics

In the early 2000s, the improper disposal and accumulation of durable petroleum-based plastics raised environmental concerns, bringing renewed interest in biodegradable plastics as an eco-friendly alternative [21]. The biodegradability of plastics relies on factors including their chemical makeup, physical form, and environmental conditions like temperature, pressure, oxygen levels, and microorganisms present. Notably, biodegradable plastics are engineered to break down under controlled settings like industrial composting facilities. If not specifically designed for environments such as soil or marine waters, biodegradable plastics may not degrade at all in those conditions, or only at a very slow pace [21].

Biodegradable polymers can be synthesized through various methods: (1) mechanochemical modification of natural polymers such as cellulose or starch; (2) chemical synthesis from monomers produced through biotechnological conversion of renewable feedstocks (e.g. lactic acid fermented from sugars); (3) chemical synthesis from monomers derived from non-renewable resources (e.g. polyvinylalcohol or PVA); and (4) direct bacterial synthesis and production of polymers (e.g. PHAs).

During processing, biodegradable plastics require careful control of parameters like temperature and moisture content to avoid issues like uncontrolled viscosity reduction, foaming, or accelerated hydrolysis [21]. Key applications for biodegradable plastics include single-use items where biodegradability is advantageous, such as packaging, food service wares, agriculture films, and biomedical implants and devices [21].

The next three paragraphs summarize the three most industrially relevant bioderived and biodegradable biopolymer classes, i.e., PLA, PHAs, and starch, highlighting the production routes, the main thermomechanical properties, and the most diffused applications. For a broader introduction to the topic of bioplastics, the reader can refer to a previous work of our group, reviewing the end-of-life strategies for bioplastics [23].

2.1.1. Polylactic acid (PLA)

PLA has become one of the most extensively used and promising biodegradable bioplastics in recent years [21]. PLA was first synthesized back in 1932 by the chemist Carothers at DuPont, but it did not reach large-scale industrial production as a bio-based and biodegradable polymer until the late 1990s [21]. PLA is an aliphatic polyester produced through the polymerization of lactide, a cyclic compound formed by the condensation reaction of two lactic acid molecules, in turn derived from the fermentation of glucose from renewable plant sources [24,25].

Lactic acid exists as two distinct optical isomers: L-lactic acid and D-lactic acid. This gives rise to three different lactide isomer forms when two lactic acid molecules condense: L-lactide, D-lactide, and *meso*-D-L-lactide [26,27]. Polymerizing the L-lactide or D-lactide isomers individually generates the semi-crystalline polymers poly(L-lactic acid) (PLLA) and poly(D-lactic acid) (PDLA) [28,29]. Commercially produced PLA typically contains mostly PLLA with a small percentage (2–4%) of D-lactide added [30]. In contrast, polymerizing the meso D-L-lactide isomer results in the amorphous polymer poly(D-L-lactic acid) or PDLLA [31,32].

The time frame for PLA biodegradation in the open environment (non-controlled degradation conditions) depends on several factors like product size, shape, optical purity, and temperature [33]. PLA exhibits good thermomechanical properties analogous to PET and PP, although inherent drawbacks like brittleness and moisture absorption exist [34–36]. Mechanical performance also relies on processing aspects including annealing, orientation, and degree of crystallization [7,21]. Leveraging its beneficial properties like high strength and clarity, PLA sees extensive use for single-use food packaging and service wares. It is also utilized for textiles, agricultural films, foams, and other applications [37–42].

2.1.2. Polyhydroxyalkanoates (PHAs)

PHAs are a family of biodegradable, bio-based aliphatic polyesters [7,36]. They are produced by polymerizing hydroxyalkanoic acid monomers with alkyl side chains containing β-, γ- or δ-hydroxyl groups. These monomers are derived from fermenting sugars and oils from renewable feedstocks using bacteria [43–45]. By changing bacteria and fermentation conditions, over 150 monomers can be incorporated to make PHA homopolymers and copolymers with different properties [46–48].

PHAs form as carbon/energy storage compounds in bacteria under nutrient-limited, high-carbon conditions, reaching high intracellular levels. However, large-scale production requires expensive fermentation and purification steps. Improvements in efficiency and cost reduction are needed for full PHA commercialization, though production capacity is rapidly increasing [49–52].

The general chemical formula of PHAs is reported in Fig. 2. Common PHAs include poly(3-hydroxybutyrate) (PHB) and copolymer poly(3-hydroxybutyrate-*co*-3-hydroxyvalerate) (PHBV). PHB is brittle with difficult processing, while PHBV, commercially available with a hydroxyvalerate (HV) content of up to 15%, shows enhanced flexibility and a lower processing temperature than PHB. A further toughness increase would be achieved by increasing the HV content, but the excessive production cost makes this pathway not yet feasible [21]. Like PLA, PHAs have potential uses in packaging and biomedical applications as bioresorbable implants or scaffolds, owing to their biocompatibility [44,53]. An advantage of PHAs is the tenfold biodegradation rate in marine environments compared to PLA: after one year in a marine environment at 30 °C, PHBV is degraded at 80%, while PLA only at approx. 8% [9].

2.1.3. Starch-based plastics

After cellulose, starch is the most abundant organic compound on Earth [46]. It is a carbohydrate produced by plants as an energy reserve and consists of two glucose polymers - linear amylose (Fig. 2) and highly branched amylopectin. Commercial starch comes chiefly from crops like wheat, rice, corn, potato, and barley. Starch makes up 60–90% of these plants' dry weight [54].

Starch's abundance, low cost, and biodegradability make it attractive for sustainable plastics [15,55,56]. Native starch must be modified using plasticizers and thermomechanical processing to

become thermoplastic starch (TPS) capable of being melt-processed like conventional plastics [15,57–60]. TPS can be tailored by blending and additives to achieve desired properties like stiffness and water resistance. Fast-degrading starch plastics are used for bags, trays, films, and other single-use items where biodegradability is advantageous [56,61].

3. Biopolymer blends

The literature defines a polymer blend as a mixture of at least two macromolecular substances, polymers, or copolymers, at over 2 wt% concentration [62]. The rising interest in polymer bends relates to the ability to develop novel polymers with customized properties different from those of the components, solving issues around synthesizing new matrices at a considerable economic advantage [63–65]. In other words, polymer blend technology can provide materials with the full desired property set at a lower cost, also offering an innovative recycling approach for industrial and municipal plastic waste. Manufacturers are interested in the potential for improved processability and versatility, reducing the grades needing production and storage. These factors explain the prevalence of polymer blends (36%) and composites (39%) in the global plastic market. Polymer companies develop around 65% of blends, compounders 25%, and transformers the other 10% [62,66].

Generally, five manufacturing methods can produce these blends: melt compounding, solution blending, latex mixing, partial block/graft copolymerization, and interpenetrating polymer network synthesis. Mixing the molten blend components via extruders or compounders is by far the most common technique given the defined constituents and versatile mixing devices. However, this approach requires high energy input and typically cannot chemically modify the components [67].

3.1. Specificity of biopolymer blends and main goals of blending

The primary motivation for blending polymers can vary greatly, from decreasing costs to enhancing mechanical attributes like impact resistance. Some of the most frequent motivations are listed in Table 1, together with several examples of biopolymer blends. Although the reported examples are derived more from the literature than from the products available on the market, the reader can refer to two recent reviews [68,69], which also list commercial biodegradable blends and products based on biopolymer blends.

The approaches taken when blending different polymers reveal the most vital properties in need of improvement. For example, PHAs are extremely adaptable but costly, so mixing them with starch aims to cut material expenses. This tactic can also be seen with PLA, although toughening through adding elastomers appears more significant, keeping an eye on the preservation of biodegradability and composting ability. Starch is inexpensive, yet has subpar mechanical abilities and is water-sensitive, so elevating those characteristics is very important. Successful blends should either perform similarly to the original material but cheaper or deliver high added value.

Generally, the properties of brittle biopolymers such as PLA and PHB are quite similar to polystyrene (PS), a popular commodity plastic. Since poor impact strength led to many PS blends and copolymers to fix this weakness, such as the widely used high-impact polystyrene (HIPS), a comparable trend is expected for PLA and other biopolymers as well. Notably, yearly publications on PS blends peaked around 2004, while interest in biopolymer blends continues rising [20].

Biopolymer blends exhibit behavior distinct from commodity polymer blends, bearing greater similarity to engineering thermoplastics. This divergence stems from the polar functional groups present in biopolymers, enabling stronger induced dipole and dipole-dipole intermolecular interactions. Such specific interactions are absent in nonpolar polymers like polyolefins, where only nonspecific dispersion forces act between chains. Consequently, the mutual miscibility between the phases is potentially greater in some biopolymer blends compared to conventional plastics.

Various studies have claimed complete miscibility in specific biopolymer blends at up to 10–20% of the dispersed phase concentration. However, rigorous quantitative determination of the actual solubility limits between biopolymer phases using thermodynamic models is rarely performed. Instead, the common inference of miscibility relies on analysis techniques like differential scanning calorimetry (DSC) and dynamic mechanical thermal analysis (DMA), through the characterization of component glass transition temperatures (T_g). Observation of a single intermediate T_g between the values of the neat biopolymers is frequently taken as evidence of miscibility. However, this criteria has limitations for accuracy when the individual T_g values are within 20–30 °C, precluding clear resolution of separate transitions [20].

More robust quantitative analysis applying models like the Kim-Burns equation [103] (see Section 5.4) to composition dependence of the glass transition could estimate miscibility, but qualitative interpretations of T_g changes currently still prevail. Complementary characterization by vibrational spectroscopy has also been undertaken to probe intermolecular interactions, through shifts in absorption bands corresponding to specific functional groups. However, the relatively weak nature of noncovalent interactions in many biopolymer blends renders such spectral shifts challenging to conclusively detect and quantify.

Approaches including the Nishi-Wang model [104] based on melting point depression (see Section 5.4) have also been applied to quantify interaction strengths and thermodynamic miscibility in semi-crystalline biopolymer blends. However, biodegradable polyesters often exhibit slow crystallization kinetics, resulting in cold crystallization during DSC measurements on initially amorphous samples. This post-processing crystallization provides little insight into equilibrium miscibility or properties, though its kinetics can reflect mobility changes. Overall, no single technique provides a sufficient understanding of miscibility and interactions in biopolymer blends. Instead, a holistic approach combining multiple complementary techniques is essential to develop robust molecular-level insight into factors controlling blend compatibility, structure, and properties [20].

3.2. Miscibility and compatibility

Although blending is an effective, economical approach to obtaining multifunctional, high-performance materials, polymer blends often have coarse phase morphology and limited interfacial adhesion between components, which occurs because most polymer pairs are immiscible. Hence, compatibilization techniques are often adopted to improve the second phase size and distribution, the interfacial adhesion, and ultimately the macroscopic physical-mechanical properties, thereby achieving the primary goals of blending. Before continuing the discussion about the compatibilization strategies, it is very important to clarify the difference between miscibility and compatibility.

Miscibility is a thermodynamic term that describes the behavior of a polymer pair by specifying the number of phases and their composition upon blending, often using the Flory-Huggins lattice model [62]. All polymers have some mutual solubility and miscibility depending on interactions characterized by parameters like the Flory-Huggins interaction parameter (χ_{12}) (see Section 3.2.1), which, despite the complexity, is still the simplest and the most

Table 1
Recent examples of compatibilized biopolymer blends.

Main polymer phase	Second polymer phase and relative amount	Type and amount of compatibilizer	Target properties to improve	Notes	Ref.
Non-reactive compatibilization					
Starch	Zein protein, 10–30%	1-butyl-3-methyl imidazolium chloride ([BMIM]Cl) ionic liquid, 23 wt%	viscosity ratio, mechanical properties	[BMIM]Cl reduces viscosity, enables finer dispersion of zein, and improves mechanical properties	[70]
PBAT	whey protein isolate thermoplastic (WPIT), 10–30 wt%	PEG, 35 wt% (of WPI)	Oxygen barrier, mechanical properties	Partial miscibility, plasticizer exudation	[71]
PLLA	NR, 4 wt%	LNR, 6 wt%	Tensile and impact strength	LNR acts as a compatibilizer to improve the interfacial adhesion of the PLLA/NR blend. The tensile strength increased by 64% and impact strength by 50% with LNR addition	[72]
PLA	PBAT, 30 wt%	PLA-PBAT-PLA triblock copolymer, 1–5%	Mechanical properties, thermal properties	Using long PLA blocks in triblock copolymer more effective than short blocks	[73]
PLA	PBAT, 20 wt%	MAM triblock copolymer	Impact toughness, elongation at break	MAM acts as compatibilizer and toughening agent, synergistic effect with PBAT	[74]
PLA	PBA, 10 wt%	PCL-b-THF 5%	Biocompatibility, biodegradability	–	[75]
PLA	NR, 10 wt%	NR-g-PLA graft copolymer, 1–5%	Impact strength	Longer grafting reaction time and higher temperature increase graft copolymer formation	[76]
Reactive compatibilization					
PLA	PBAT, 30 wt%	E-GMA, 6%	Elongation at break and tensile strength	Compatibility between PLA and PBAT improved but impact strength not measured	[77]
HDPE	Tapioca starch 20–40%	PE-g-MA 5–15% based on starch	Thermal stability, mechanical properties	Moisture sensitivity	[78]
PLA	NR, 5–15 wt%	epoxidized and acetic acid modified NR	Toughness, strength	Decreased strength with increasing natural rubber content	[79]
PLA	Novatein, 10–50 wt%	PLA-g-itachonic anhydride	foamability and pore morphology of PLA	Presence of novatein crystalline regions reduces CO2 solubility, leading to non-uniform CO2 distribution. Compatibilization with PLA-g-IA can increase PLA crystallinity, also restricting cell growth.	[80]
LDPE	Chitosan, 20–60 wt%	Glycidyl methacrylate grafted LDPE (PEGMA), up to 12% of chitosan amount	Mechanical properties, biodegradability	Not significant improvement in mechanical strength and reduction in elongation at break due to rigid chitosan phase compared to neat LDPE	[81]
PLA	Epoxidized natural rubber (ENR), 10–30 wt%	ENR-g-MA graft copolymer, 0.15–0.6 phr	Impact strength, thermal stability	Higher MA concentration increases grafting reaction and compatibility. Tg of PLA decreased while Tg of ENR increased.	[82]
PLA	PP, 30 wt%	Ethylene-butyl acrylate-glycidyl methacrylate terpolymer (EBA-GMA), 2.5–10 wt%	Tensile strength, impact strength	EBA-GMA effective for improving tensile and impact strength but decreases tensile strength at high loading; Co-continuous morphology enables improved properties	[83]
PLA	PBAT, 20 wt%	PLA-g-TPU graft copolymer, 10%	Extrusion behavior, thermal stability, impact strength	Graft copolymer improved compatibility and phase adhesion	[84]
PLA	PHBV, 10–40 wt%	Peroxide initiator (0.1–0.5 wt%)	Elongation at break, tensile strength	Excessive initiator can reduce elongation at break	[85]
PLA	PCL, 50 wt%	Vinyl functionalized graphene (0.5–2 wt%)	Tensile strength, elongation at break	Addition of initiator can reduce elongation at break	[86]
PLA	PBAT, 10 wt%	PLA-g-MA 3–9% based on PBAT	Tensile strength, elongation at break, impact strength	Possible decrease in elongation and impact strength at high loading of compatibilizers	[87]
PLA	PPC, 30 wt%	POE-g-GMA, 1–7 wt%	Toughness, melt strength	Tensile strength decreased, excess epoxy groups caused embrittlement	[88]
PHBV	PLA, PBAT (1:1:1 ratio)	epoxy-based styrene–acrylic oligomer (ESAO), 2 phr	Mechanical properties, barrier properties	Poor thermal stability of PHBV	[89]
PBS	PPC, 25 wt%	gPPC, 5–25 wt%	Elongation at break	Tensile strength decreased at high gPPC	[90]
Bio-HDPE	PLA, 5–20 wt%	PE-g-MA, 3 phr; PE-co-GMA, 3 phr; Maleinized linseed oil (MLO), 5 phr; MLO + dicumyl peroxide (DCP), 5 phr +1 phr	Mechanical strength, rigidity, toughness, thermal stability	Use of MLO and DCP gave the best balance of mechanical performance	[91]
TPS	PBAT, 40 wt%	Maleic anhydride (MA), 2–6 wt% Citric acid (CA), 2–6 wt%Maleated PBAT (PBATg-MA), 2 wt%	Mechanical properties, morphology	Addition of MA or CA over 2 wt% negatively impacted mechanical properties	[92]
PLA	PBAT, 10 wt%	EMA-GMA, 8–15 wt%	Impact strength	PLA crystallinity decreased with compatibilizer addition	[93]

PLA	PBAT, 20 wt%	DCP, 0–1 wt%	toughness, hydrolytic degradation	in-situ compatibilization improves toughness but not hydrolytic degradation	[94]
PLA	TPU, TPE (10 phr)	5 phr PLA-g-MA	Toughness, thermal stability, rheology	Decreased domain size with PLA-g-MA	[95]
PLA	PBAT, 30 wt%	MPEG-PLA block copolymer, 12% total MPOE and GPOE	Viscoelasticity, film stretching ability	Long chain branching formed, uniform and toughened PLA film obtained	[74]
PLA	TPS, 20%	GMA, 1%; BPO, 0.1%	Biodegradation rate	Starch component degrades rapidly leaving voids in the material	[96]
Nanofiller-induced compatibilization					
PLA	PBAT, 20–40 wt%	CNTs, 0–4 wt%	Impact strength, electrical conductivity	the yield strength decreased upon the addition of CNTs	[97]
PLA	PCL, 20 wt%	ZnO nanoparticles (2–6 wt%)	Thermal and hydrolytic degradation	ZnO introduced accelerated degradation of PLA/PCL blend; no mechanical properties assessment	[98]
PLA	PCL, 30 wt%	Cellulose nanocrystals grafted with PLLA or PCL chains, 1%	Shape memory properties	Addition of grafted nanofillers did not significantly affect shape memory response compared to neat blend	[99]
PCL	PLA, 30 wt%	CNTs and organoclay, 0.5% each	Mechanical properties, thermal stability	Synergistic effect between CNTs and organoclay	[100]
PLA	TPU, 30 wt%	CNTs, 2%	Impact strength	CNTs confined in TPU phase induced physical crosslinking	[101]
PCL	PLA, 30 wt%	Carbon nanotubes, 0.5–1 wt%; Organically modified montmorillonite, 0.5–1 wt%	Elongation at break, tensile strength, thermal stability	Synergistic effects between nanofillers	[102]

widely used practical approach. However, few papers quantitatively correlate miscibility, structure, and properties, although these important correlations exist. This topic will be described more in detail in Chapter 5.

On the other hand, compatibility is a technical term defining the blend's property profile for an application. If the property combination is advantageous, the polymers' compatibility is good. They are incompatible if properties are unacceptable [20]. Compatibility is often modified physically (compatibilizers, block copolymers, nanofillers) or chemically (reactive processing). The most important compatibilization strategies adopted for biopolymer blends are described in Chapter 4. It is important to underline that the goal of such compatibilization strategies is often not to achieve full miscibility, but to tailor the microstructure and the interfacial adhesion so that the target macroscopic properties are optimized.

3.2.1. Thermodynamics of miscibility

The thermodynamic miscibility of two polymers is determined by the change in Gibbs free energy of mixing (ΔG_{mix}) that occurs upon blending. If ΔG_{mix} is negative, the blend will be miscible as mixing is energetically favorable. Conversely, a positive ΔG_{mix} indicates an immiscible blend. The Flory-Huggins lattice theory provides a quantitative framework to calculate ΔG_{mix} based on the combinatorial entropy of mixing and enthalpic interactions between polymer segments [105]:

$$\Delta G_{mix} = RT(n_1 \ln \varphi_1 + n_2 \ln \varphi_2 + \varphi_1 \varphi_2 \chi_{12}) \quad (1)$$

where n_1 and n_2 are the degree of polymerization of polymers 1 and 2, φ_1 and φ_2 are the volume fractions of each polymer, R is the gas constant, and T is the absolute temperature.

The key parameter in this equation is χ_{12}, the Flory-Huggins interaction parameter. This quantifies the enthalpic interactions between polymer 1 and polymer 2 segments on a lattice. A smaller, more negative value of χ_{12} indicates stronger, more favorable inter-polymer interactions that increase miscibility. In contrast, a larger, more positive χ_{12} signifies weaker interactions and decreased miscibility.

The χ_{12} parameter incorporates the Hildebrand solubility parameters (δ) of each polymer [106], according to Equation (2):

$$\chi_{12} = \frac{V}{RT}(\delta_1 - \delta_2)^2 \quad (2)$$

where V is the reference volume, usually taken as the molar volume. The Hildebrand solubility parameter represents the total cohesive energy density for a polymer, arising from all intermolecular interactions including van der Waals forces, hydrogen bonding, and dipole-dipole interactions. Polymers with similar δ values have similar cohesion energies. Consequently, blending polymers with similar Hildebrand parameters results in a smaller enthalpic penalty upon mixing, reducing χ_{12} and increasing miscibility. Hence, the miscibility between polymers can be assessed via the critical solubility parameter difference $\Delta\delta_{crit}$, as per the approach described by Coleman et al. [107]. A recent example of this approach is presented in the work of Tuancharoensri et al. [108], who determined the $\Delta\delta_{crit}$ to investigate the miscibility of ternary PLA/PCL/cellulose acetate butyrate (CAB) biopolymer blends.

In summary, the Flory-Huggins lattice model relates the molecular characteristics of two polymers to their thermodynamic miscibility through the interaction parameter χ_{12}. Polymer pairs with similar Hildebrand solubility parameters will have favorable inter-polymer interactions, a lower χ_{12}, and greater miscibility. This theoretical framework allows the prediction and interpretation of

phase behavior in polymer blend systems. The model can be extended to multicomponent blends and copolymers for an even deeper understanding of polymer mixture thermodynamics.

Since miscibility in polymer blends requires a precise combination of conditions (polymeric phase configuration, molecular weight/distribution, temperature, pressure, stress field, additives, etc.), most commercial blends are immiscible. Additionally, blend macroscopic properties strictly depend on morphology. This means that the microstructural features must be stable, predictably affected by processing, and reproducible. Thus, compatibilization is the most widely used technique to achieve these effects.

3.3. Examples of industrially relevant biopolymer blends

The open scientific literature abounds with examples of biopolymer blends, demonstrating the increasing academic and industrial interest in this topic. Among all the reported cases, two blend groups deserve to be examined more closely because of their significance and industrial relevance: (i) starch blends and (ii) impact-modified PLA and PHAs.

3.3.1. Starch-containing blends: decreased cost and acceptable properties

For biopolymers, cost is always critical: their price generally exceeds that of commodity plastics, thus hindering their practical application. On the other hand, starch is inexpensive and abundant, and is being increasingly used in blends and composites to reduce prices of other bio-based/biodegradable polymers like PLA and PHAs [20].

Two approaches produce starch-based heterogeneous systems [19]. One uses neat or chemically modified starch particles to make composites. Strong hydrogen bonding in native starch hinders particle dispersion on molecular and microscopic scales, yielding composites rather than blends, but they generally show very poor properties. Moreover, several starch blends with traditional petrochemical polymers were previously reported as biodegradable but failed to meet modern requirements: they do disintegrate due to starch degradation, but the conventional polymer rarely degrades. Today, traditional polymers are generally blended with starch to decrease the fossil-based content [109,78], but the true ecological advantage across the whole life cycle of this approach is yet to be fully understood. The other approach is thermoplastic starch (TPS) from plasticization with water or glycerol, offering much better properties [92,110].

Commercial biopolymer/starch blends are available, but decreased cost from starch usually impairs other characteristics. With poor miscibility, blending often reduces mechanical properties versus both components. Thus, the main starch blending goal is to minimize cost while maintaining acceptable properties. Additionally, it is generally very difficult to predict and model the properties of these blends, as the Interactions and microstructure are extremely complicated, with plasticizer partition in both phases and the frequent need for compatibilization further hampering predictions [111,112].

3.3.2. Toughening brittle biopolymers through blending

Blending brittle biopolymers with elastomers can create tailored, bio-based/biodegradable impact-resistant materials. Like starch, improving PLA impact strength has been a key objective using biopolymers including PBAT, starch, thermoplastic polyurethane (TPU), furanoate polyesters, PE, poly(ethylene octene) (PEO), poly(propylene carbonate) (PPC), natural rubber (NR), tough PHA copolymers, PBS, and PCL [34,40,74,75,77,85,87,88,91,102,113–119]. For PHB, copolymerization with longer side-chain hydroxyalkanoates usually addresses brittleness. However, effective blending approaches exist and should not be overlooked for potential engineering and economic benefits [111,83,89,120–123]. Most aforementioned blends have low miscibility and interfacial interaction, needing proper compatibilization to avoid inferior mechanical properties.

In summary, biopolymers' vast chemical diversity enables unlimited property modification potential through blending. Interactions play a crucial role in determining blend structure and properties, necessitating a more thorough consideration of miscibility-structure-property correlations to fully utilize this potential. Despite the polar character of biopolymers, compatibilization is often still needed to achieve application-specific properties.

4. Compatibilization strategies for biopolymer blends

Compatibilization is indispensable for realizing the full potential of biopolymer blends and enabling their widespread adoption as sustainable alternatives to petroleum-derived plastics. The inherent immiscibility between biopolymers, arising from unfavorable mixing entropy, leads to phase separation and coarse morphologies when blended. This results in poor mechanical properties, instability, and phase coarsening over time that restrict applicability. Compatibilization aims to address these challenges through physical or chemical modification of interfacial interactions to obtain intimate mixing, stable microstructure, and a synergistic combination of the complementary properties of the biopolymers [62].

The main objectives of a compatibilization strategy are reducing the interfacial tension, stabilizing the fine morphology against coarsening, and improving interfacial adhesion between the phases [124]. Interfacial tension reduction to obtain finer dispersed phases is readily achieved by the addition of macromolecular ‘surfactants’. However, more crucial is enhancing adhesion in the solid state to retain fine morphology and enable efficient stress transfer. Compatibilizer design and selection focuses on enabling these effects.

Different strategies can be adopted to reach proper compatibilization, and the suitability of a compatibilization technique at the industrial level is strongly related to many aspects, such as cost, final performance, recyclability, and possible biodegradability. The strategies are divided mainly into three groups: (i) non-reactive compatibilization, relying on co-solvents or block- or graft-copolymers; (ii) reactive compatibilization, in which the copolymer is formed in situ during processing; (iii) nanofiller-induced compatibilization, which relies on the addition of a small amount of nanofillers [62,107].

Block copolymers with each block miscible in one phase represent the most explored physical compatibilizers for biopolymer blends. The anchored blocks provide coupling while the stretched mid-block provides a gradient interphase. However, limitations like phase inversion instability and high cost have restricted their broad applicability. Alternative physical methods using small molecules, nanoparticles, or homopolymers have shown only limited success so far. Instead, chemical reactive compatibilization proves far more effective than physical blending. Mutually reactive polymers can be added to create grafted compatibilizers in-situ. Alternatively, reactive extrusion modifies the blend components via reactions between inherent reactive groups or added reactants, generating interfacial compatibilizing moieties. The abundance of reactive groups makes many biopolymers amenable to such reactive strategies. Nanoparticle addition also compatibilizes blends by localizing at interfaces, interacting strongly with the phases [19,62,125].

While compatibilizer design is crucial, optimizing melt-mixing parameters like temperature, shear rate and time offers further control over the blend morphology. Shear forces during mixing

break up the dispersed phase into smaller domains, with the equilibrium size determined by viscosity ratio, elasticity, and interfacial interactions. Higher shear and stronger interfacial adhesion provide the finest dispersions, enhancing properties. However, processing alone cannot induce the interphase interactions necessary for optimal performance. Its effects synergistically complement chemical or physical compatibilization. Proper design and selection of a compatibilization strategy are thus pivotal to developing high-performance materials by blending immiscible biopolymers. However, challenges remain in comprehensively understanding the interplay between compatibilizer chemistry and localization, processing conditions, evolving morphology, and final properties. Systematic fundamental and applied research in this area will pave the way for economically viable biopolymer blend systems with tailor-made structures and properties.

In the rest of this Chapter, the three main strategies for biopolymer blend compatibilization will be illustrated and exemplified through some recent examples from the literature.

4.1. Non-reactive compatibilization via block- and graft-copolymers

A common technique to compatibilize otherwise immiscible polymer blends involves adding a third polymeric component, typically a block or graft copolymer, with segments identical or similar to the two parent polymers [62]. It is critical that such copolymer segments can create specific interactions like hydrogen bonding, ion-dipole, dipole-dipole, or Lewis acid-base interactions with the two polymer constituents. To be effective, this compatibilizer must be able to migrate to the interface to modify rheological behavior and reduce interfacial tension, thereby reducing the coalescence of the minor phase domains (Fig. 3) and stabilizing the morphology [126].

Effective compatibilization requires the copolymer to have high miscibility with both polymer components of the blend. Additionally, the copolymer should have a limited molecular weight around the entanglement value for each interacting segment and it should be effective already at a low concentration in the blend (0.5–2 wt%) [62]. To assess compatibilization efficiency, mechanical properties sensitive to stress transfer like impact strength, tensile strength, and elongation at break are useful, as they indirectly indicate interfacial adhesion [127]. Utracki's book [62] provides a thorough analysis of the thermodynamics of copolymer-compatibilized blends and commercial examples. Furthermore, Fortelny's review details the effects of block and graft copolymers on phase structure formation and evolution in immiscible blends [128].

For example, Mo et al. [84] investigated using PLA-g-TPU (PGU) graft copolymers to compatibilize and improve the properties of PLA/TPU blends. The graft copolymers were synthesized by melt mixing PLA, dicumyl peroxide, glycidyl methacrylate, and TPU. The compatibilization effect on PLA/TPU blend morphology and properties was studied for different graft copolymer contents. SEM showed the TPU domain size decreased from 2 μm to 0.3 μm with graft copolymer addition, indicating improved compatibility. The graft copolymer also enhanced thermal stability and mechanical properties. As shown in Fig. 4, the strain at break increased from 11.2% for the blend to 87% with 10 wt% graft copolymer. The tensile strength also increased from 44.7 MPa to 53.4 MPa (+16%) at optimal graft content. The improved interfacial adhesion between PLA and TPU phases led to simultaneous toughness and strength enhancement. The authors credited the enhanced interfacial adhesion between the PLA and TPU phases, provided by the tailored graft copolymer, for this increase in tensile strength. The compatibilization enabled more effective stress transfer across the

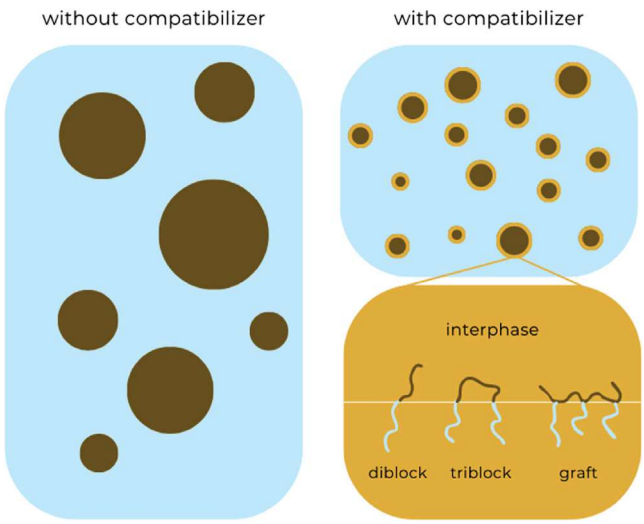

Fig. 3. Compatibilization of a polymer blend with graft- and block-copolymers (adapted from Ref. [19]).

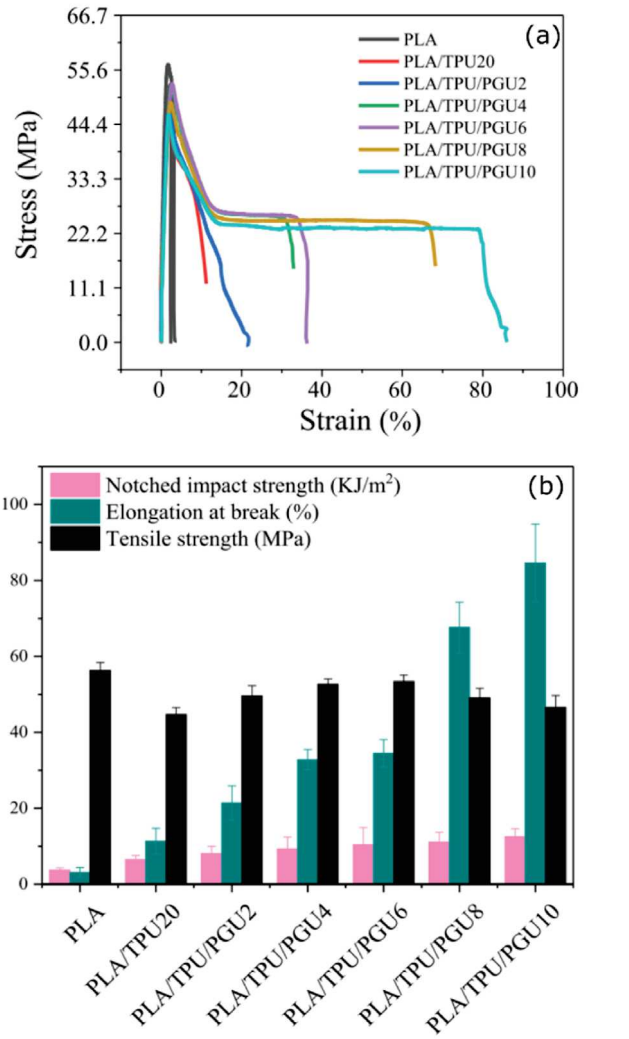

Fig. 4. (a) Stress-strain curves of PLA, PLA/TPU20 blends, and PLA/TPU/PGU blends; (b) Mechanical properties of PLA, PLA/TPU20 blends, and PLA/TPU/PGU blends (duplicated with permission from Ref. [84]).

interface, strengthening the blend. However, the authors did not report any information about the accompanying variation (possibly reduction) in stiffness with increasing TPU content.

In another work, Ding et al. [129] studied using monomethoxy poly(ethylene glycol)-polylactide (MPEG-PLA) di-block copolymers to compatibilize PLA blends with PBAT, PBS, or poly(butylene succinate-*co*-adipate) (PBSA). The copolymers were synthesized by ring-opening polymerization of lactide initiated by MPEG under catalytic tin octoate at 135 °C for 24 h. The PLA block length was controlled by the ethylene glycol (EG) units from the MPEG block to lactic acid (LA) units in the PLA block of the di-block copolymer (EG/LA ratio). Copolymers with tailored EG/LA ratios were prepared and characterized by nuclear magnetic resonance (NMR), DSC, and size exclusion chromatography (SEC). Scanning electron microscopy (SEM) showed the di-block copolymers reduced the dispersed phase size from 2 μm to 0.3 μm in PLA/PBAT, indicating improved compatibility. The copolymers also enhanced PLA crystallinity and modified blend rheology. Mechanical testing demonstrated significantly improved ductility and toughness: the strain at break of PLA/PBAT increased over 10 times with 3 wt% copolymer added, reaching 296%. The PEG segments enabled miscibility with PLA and the other polyester phase, while the PLA block provided compatibility with the PLA homopolymer, and also for other polyesters the strain at break was increased (Fig. 5a and b). The addition of 3% ME91L18 di-block copolymer, having a degree of polymerization of the MPEG block of 91 and the PLA block of 18, increased the tensile strength of the PLA/PBSA blend from 32 MPa to 43 MPa. The authors attributed this 21% increase in tensile strength to stronger interfacial adhesion between the PLA and PBSA phases provided by the optimized di-block copolymer structure (Fig. 5c and d). However, also in this case, the paper does not provide quantitative information on how the compatibilization affected the stiffness of the blends, as data on elastic modulus are not reported.

Although compatibilization aims to improve performance, its effect on mechanical properties is often overlooked. Many authors infer the success of the compatibilization strategy from changes in thermal behavior or morphology. These properties do offer insights into miscibility, but successful compatibilization relates to advantageous property changes for certain applications. Regrettably, physical, non-reactive compatibilization has limitations, as substantial, simultaneous improvements in strain at break and mechanical strength via physical compatibilization are generally rare. In contrast, much greater effects occur with reactive techniques, which allow tuning the properties over a much broader range, expanding the applicability of biopolymer blends [20].

4.2. Reactive compatibilization

The reactive compatibilization technique directly forms graft or block copolymers in situ during melt blending to serve as

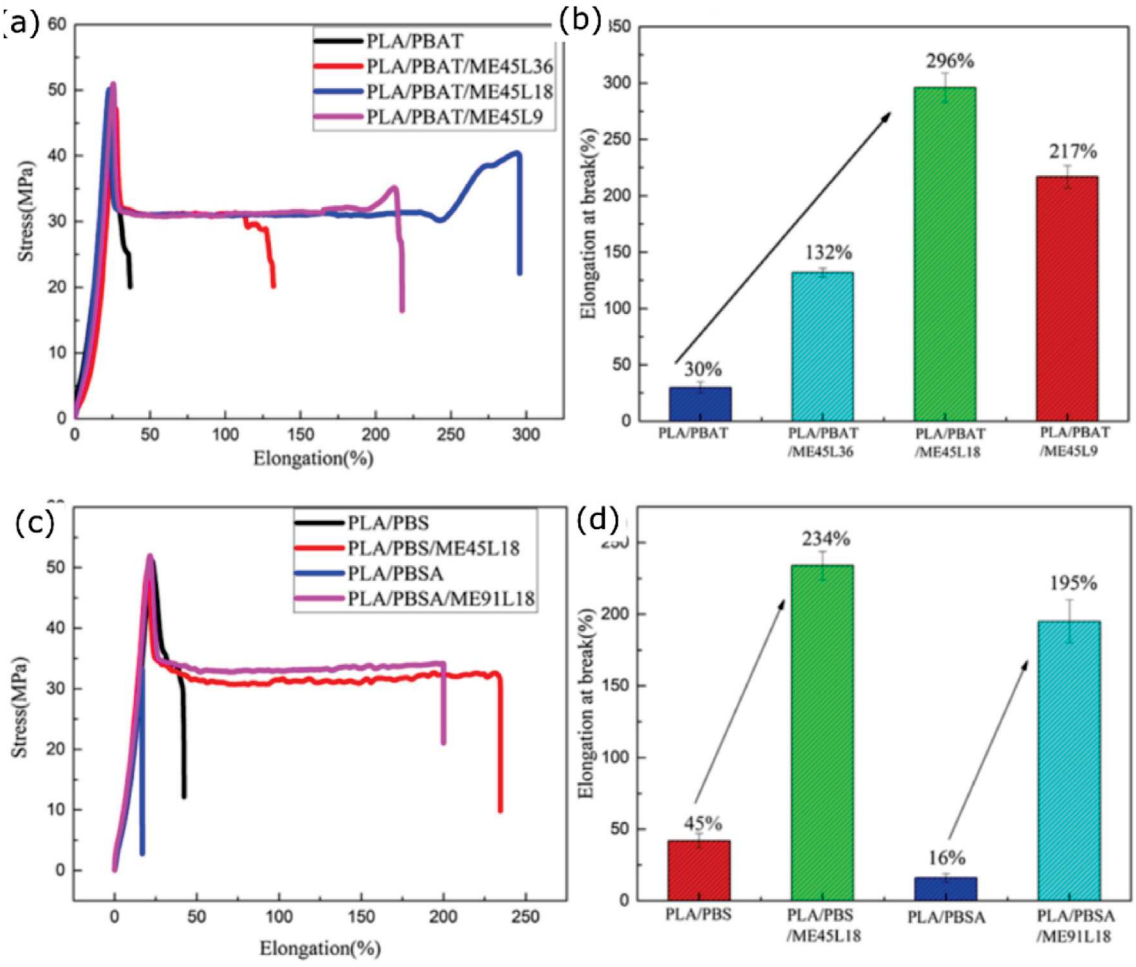

Fig. 5. (a) Stress-strain curves of the PLA/PBAT blends with compatibilizers and (b) the elongation at break of the PLA/PBAT blends with compatibilizers. (c) Stress-strain curves of the PLA/PBS and PLA/PBSA blends with compatibilizers and (d) the elongation at break of the PLA/PBS and PLA/PBSA blends with compatibilizers. Duplicated with permission from Ref. [129].

compatibilizers. In this technique, chemical reactions between suitably functionalized polymers allow the synthesis of these copolymers right at the interface. This links the immiscible phases through covalent or ionic bonds, refining the dispersed phase and enhancing interfacial adhesion. This method intricately integrates organic chemistry and polymer processing, as it connects chemical reaction kinetics to the rheological and thermal properties of the reactants and products [62].

Forming the compatibilizer in situ overcomes the transport limitations of adding premade copolymers, which gives better control over the blend microstructure. Efficient reactive compatibilization uses fast, selective reactions and mixing conditions, so to minimize mass transfer constraints [64,130]. Matching the molecular weights of the copolymer blocks to the corresponding blend phase polymers is another advantage, as this optimizes interfacial adhesion. Reactive blending can also create thicker, more rigid interphases compared to adding copolymers [62].

Biopolymers often contain reactive groups that enable excellent reactive compatibilization of their blends. Adding a compound miscible with one component but reactive to the other's functional groups produces grafted or block copolymers in situ as compatibilizers. The proper selection of agents, blend composition, and processing conditions allows for controlling structure and properties. For example, grafting polymers with anhydrides, forming free acids, enables compatibilization of hydroxyl-rich polysaccharides [111]. Blends of starch with maleic anhydride (MA)-grafted PCL, PLA, and PHB prepared this way show improved compatibility [19,95]. In-situ synthesized block copolymers of MA-grafted PLA and hydroxyl-terminated poly(ethylene glycol) PEG also increase PEG/PLA blend compatibility. Other reactive groups like epoxides or isocyanates can couple phases [85,130,131].

Properly selecting the reactive groups and extrusion conditions is crucial. Reactive groups should readily form bonds under processing conditions without degrading the polymers. Highly efficient reactions enable the use of low compatibilizer levels, avoiding property deterioration. Extruder temperature, shear rate, and residence time must balance grafting reaction rates, adequate mixing, and minimizing degradation [89,90]. Applicable reactive extrusion reactions include (i) chain cleavage and recombination, (ii) polymer end groups reacting together, (iii) a polymer end group reacting with pendant groups on another polymer, (iv) covalent crosslinking between reactive groups on polymer main or side chains, and (v) ionic bond formation [132].

Overall, biopolymers' reactive groups facilitate compatibilization by reactive blending. With proper selection of reactive agents and processing, grafted or block copolymers generated in situ couple the phases, refining morphology and enhancing interactions and mechanical properties. However, biopolymers' specificity necessitates customizing reactive extrusion conditions to the system, balancing grafting reactions, and avoiding degradation [20,130,90].

For example, in a recent study, He et al. [77] enhanced the toughness of brittle poly(lactic acid) (PLA) films by reactive blending with low levels of poly(ethylene octene) (POE) elastomer. POE was first grafted with glycidyl methacrylate (GPOE) and maleic anhydride (MPOE) to introduce reactive epoxy and anhydride groups. GPOE and MPOE were then melt blended with PLA, enabling covalent bonding between the phases (Fig. 6a). The resulting PLA/GPOE-MPOE blend exhibited significantly increased complex viscosity, storage modulus, and strain hardening versus neat PLA, indicating improved molecular entanglement from long-chain branching. SEM showed spherical POE domains tightly embedded within the PLA matrix for PLA/GPOE-MPOE, in contrast to obvious debonding between phases in PLA/POE (Fig. 6b). Strong interfacial adhesion enabled effective stress transfer in PLA/GPOE-MPOE, evidenced by ductile impact fracture with plastic deformation rather than brittle behavior with fibrillation/debonding (Fig. 6c). In summary, grafting POE with reactive groups and then melt-blending it with PLA formed covalent linkages between phases. This compatibilization approach generated PLA/POE films with greatly enhanced toughness, enabled by tailored interfacial interactions and molecular entanglement from long-chain branching.

While reactive extrusion enables in-situ compatibilization during blend preparation, tuning processing parameters like shear rate and residence time can further enhance compatibilization synergistically. For example, Calderon et al. [90] investigated the effect of specific mechanical energy (SME) on the reaction efficiency and properties of PLA/PPC and PBS/PPC blends prepared by high-speed reactive extrusion. SME expresses the mechanical work input during extrusion.

Increasing SME, by raising screw speed at constant SME, enhanced the grafting efficiency of MA-modified PPC onto the polymer matrices. High SME also lowered PBS blend viscosity due to degradation, while modulating SME gave refined PBS morphology versus coarse, aggregated structure at very high SME (Fig. 7a). Short residence time was key; high shear treatment at short times gave only mild viscosity loss. Limited heat accumulation at short times prevented extensive degradation despite high shear rates. Mechanical properties showed residence time was more impactful than high shear for PBS blends. The highest strain at break was achieved for high shear, short time conditions once compatibilized (Fig. 7b and c). While SME trended with grafting efficiency, the rheology, morphology, and properties of the blends were quite sensitive to shear and thermal history. For PLA blends, high shear had less effect than for PBS, with properties optimized at moderate shear. This illustrates the need to tailor reactive extrusion to the polymer system.

Reactive compatibilization strategies have been also explored extensively for improving the properties of blends containing polysaccharides such as starch, cellulose, and hemicelluloses [19]. The hydroxyl-rich structure of plant polysaccharides enables a range of chemical modifications that can form amphiphilic structures for compatibilization with non-polar polymer matrices. Typical reactive approaches include graft copolymerization, coupling, and substitution reactions.

Graft copolymerization involves in-situ formation of polyester side chains on polysaccharides through ring-opening polymerization (ROP) of cyclic monomers like ε-caprolactone and lactide. This provides an efficient one-step method to introduce hydrophobic grafts compatible with aliphatic polyester matrices, generating polysaccharide-*graft*-polyester copolymers. ROP grafting is often conducted under solvent-free conditions or in ionic liquids, using organometallic catalysts like stannous octoate [99]. The molar mass and graft density can be tailored by factors including monomer-to-polysaccharide ratio, type of initiator, and reaction time.

Coupling reactions attach small bifunctional molecules or macromolecules to polysaccharides and a second polymer phase, crosslinking the interface. Examples are diisocyanates and MA-grafted polymers, which couple with polysaccharide hydroxyls and matrices like polyesters. While excessive crosslinking causes thermoset behavior, limited coupling improves stress transfer without network formation. Coupling effectiveness depends on the reactivity and number of functional groups in the agent and polymer phases [92,83].

Polysaccharide hydroxyls are frequently substituted by esterification with anhydrides, acyl chlorides, or acids, attaching hydrophobic groups like acetyl and longer alkyl chains. This disrupts polysaccharide crystallinity and reduces hydrophilicity, changing rheological properties and often improving dispersion. However, substitution also decreases interfacial interactions with the matrix

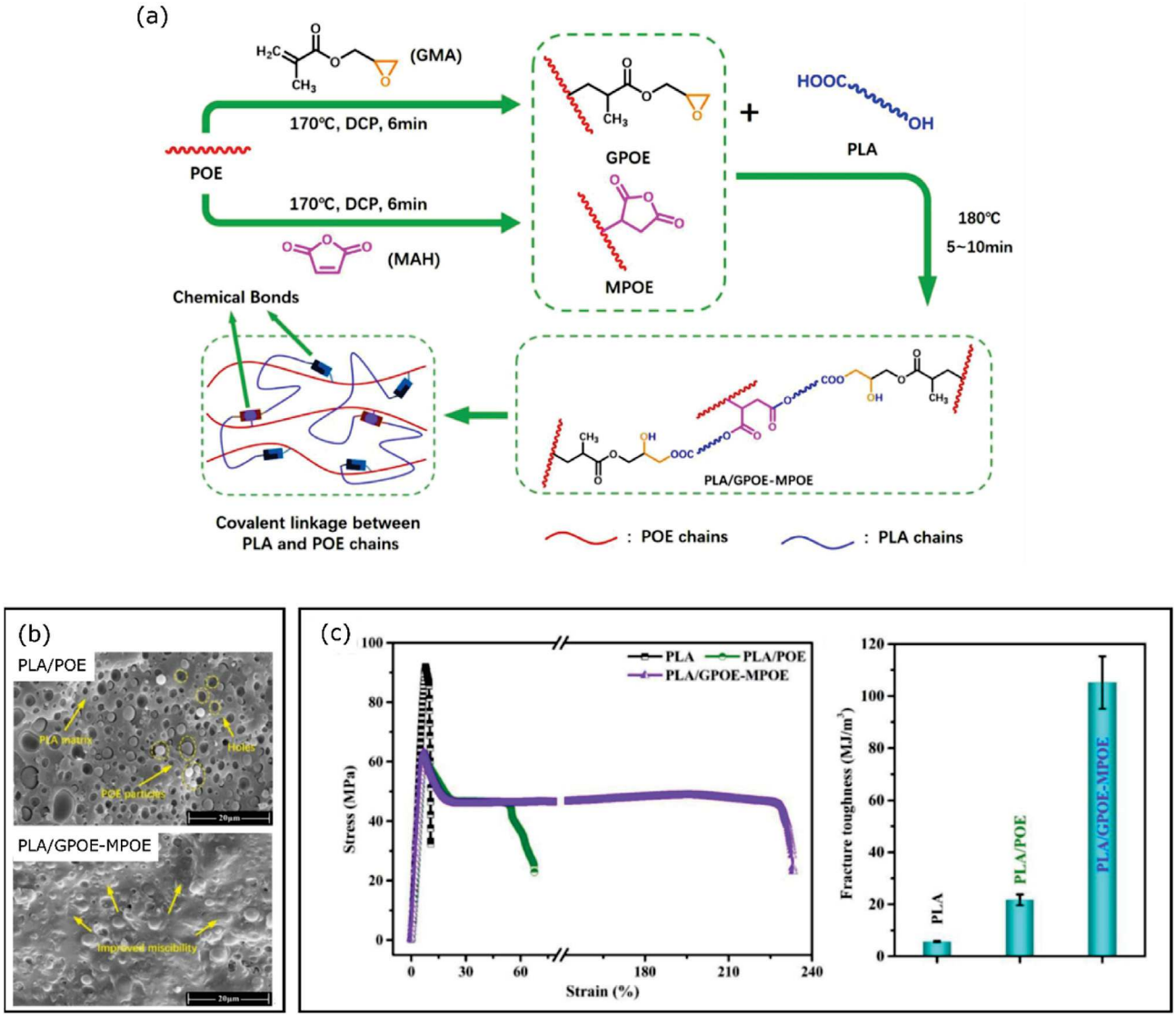

Fig. 6. Reactive compatibilization of PLA and POE. (a) Schematic illustration of the formation of interfacial covalent linkage in PLA/GPOE-MPOE blend; (b) SEM micrographs of cyrofractured PLA/POE and PLA/GPOE-MPOE blends; (c) Stress-strain curves and fracture toughness of the prepared blends. Duplicated with permission from Ref. [77].

polymer. Despite this drawback, substituted polysaccharides can enable finer morphology and tensile strength enhancements in some cases, particularly with non-plasticized starches [19,109].

4.3. Micro- and nanofiller-induced compatibilization

The previously mentioned compatibilization strategies, although effective, can be limited in versatility and require extensive changes to established industrial practices. However, recent research demonstrates that incorporating nanoscale fillers provides a versatile new approach to manipulate blend morphology and compatibilize immiscible polymers, without major modifications to mixing methods or chemistry. By localizing at interfaces and within phases, nanoparticles can profoundly alter rheological and interfacial properties governing morphology development. This allows tailoring of the microstructure to enhance blend performance, bypassing complications of conventional techniques. Owing to its simplicity and effectiveness, nanofiller-induced compatibilization has garnered great research interest in upgrading immiscible blends across various polymer systems and applications. The incorporation of nanoparticles emerges as an elegant and affordable solution to long-standing challenges in compatibilizing industrial polymer blends [125,133].

Although the same compatibilization mechanisms that will be described for nanofillers can apply to some micrometric fillers [134], the majority of the work about filler-induced compatibilization is focused on the use of nanometric or nanostructured fillers, therefore this paragraph and the presented examples will mainly concentrate on nanofillers. The nano-scale fillers can be categorized into three main groups according to their geometry [135]: one-dimensional (e.g. layered silicates, graphene nanoplatelets); two-dimensional (e.g. carbon nanotubes, nanofibers); and three-dimensional (e.g. metal oxide nanoparticles, carbon black).

A key factor determining the final composite properties is the dispersion and distribution of the nano-filler within the polymer matrix, alongside the interfacial interactions between the filler and matrix. This is because the polymer chains behave very differently at the nano-scale interfaces versus in the bulk polymer. Successful exploitation of nanocomposites therefore relies on optimizing these nano-scale interactions. In fact, nanofiller-induced

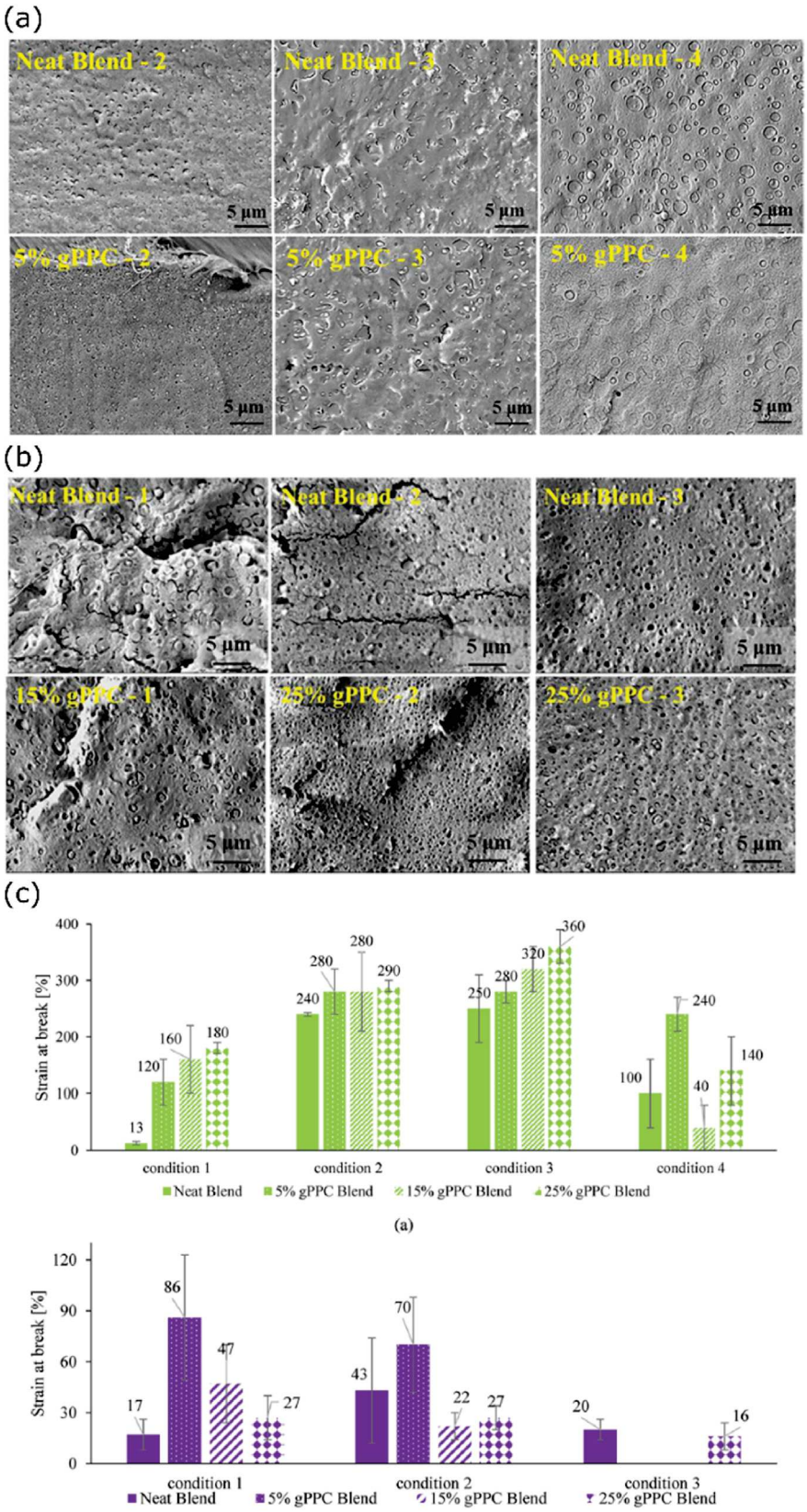

Fig. 7. SEM images of the PBS blends (a) and PLA blends (b) processed at different conditions and with or without compatibilizer. (c) Strain at break as a function of the different processing conditions and amount of compatibilizer. Duplicated with permission from Ref. [90].

compatibilization operates through various mechanisms by which the nanoparticles alter the microstructure and interactions at the polymer-polymer interface [136,101].

In addition to physical effects, chemical functionalization of the nanofiller surface can increase its compatibility with the biopolymers [86]. Many papers highlighted the compatibilization effect on polymer blends provided by the introduction of both unmodified and surface-treated nanofillers [99]. Untreated nanoparticles are preferable with high processing temperatures, so to avoid the thermal degradation of the organic modifier [137]. Moreover, the nanofiller morphology also plays a key role – high aspect ratio nanotubes or nanofibers provide connectivity between phases. By tuning nanoparticle localization and utilizing these various effects, the phase morphology can be optimized to achieve superior mechanical performance for immiscible bioplastic blends.

The addition of nanofillers to polymer blends can significantly impact crystallization behavior, with important implications for morphology, compatibility, and properties. As reviewed by Das et al., nanoparticle-polymer interactions can induce new crystal forms near the nanofiller that are absent in the unfilled blend. This localized nucleating effect alters crystallization kinetics and crystalline microstructure development, which can influence phase separation and stabilize specific morphologies. Consequently, the resulting crystal-amorphous structure in the nanocomposite blend affects interfacial interactions as well as mechanical performance. Through careful selection of nanofillers and processing conditions, control over crystallization can be a powerful tool to direct morphology and enhance compatibility in immiscible systems [138].

Beyond mechanical properties, nanofiller-guided manipulation of bioplastic blend morphology shows promise for improving other key properties like heat resistance, gas barrier, UV barrier, and flame retardancy. It also provides a pathway to finely tune morphology for applications such as membranes with controlled pore structures. Furthermore, the approach facilitates the value-addition of recycled bioplastics by enabling better blending with virgin resins [119,125].

The physical mechanisms underlying nanofiller-induced compatibilization and morphology control in phase-separating polymer blends have been explored by researchers like Lipatov, Nesterov [139], and Ginzburg [140]. In general, the compatibilizing effects stem from preferential localization of the nanofiller, which can lower interfacial tension, suppress coalescence, and refine morphology. These phenomena are encompassed in Taylor's theory [141] relating the domain size in a blend to factors including interfacial tension, matrix viscosity, and shear rate, as reported in Equation (3):

$$\sigma_{int} = \frac{\eta_m \dot{\gamma} d}{W_c} \tag{3}$$

where σ_{int} is the interfacial tension, η_m is the viscosity of the matrix (η_m), $\dot{\gamma}$ is the shear rate, d is the resulting domain size, and W_c is the critical Weber number. Hence, a decrease in the dimension of the dispersed domains is correlated with a higher interfacial area and a lower interfacial tension and therefore to a higher interaction between the constituents, with a consequent improvement in the performance of the blend.

The addition of nanofillers to increase compatibilization has been a strategy also for biopolymers, as it allows coupling the compatibilization with the improvement of other mechanical and functional properties due to the direct introduction of the nanofiller. This has been reviewed by Mochane et al. in a recent review focused on the localization of fillers and nanofillers in biopolymer blends [136].

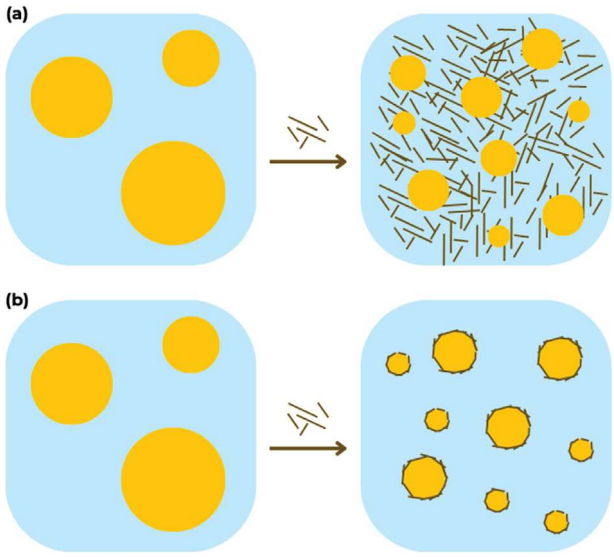

Fig. 8. Scheme of the two main strategies of nanofiller-induced compatibilization based on the selective localization of the nanofiller (a) nanofiller preferentially dispersed in one of the two phases; (b) nanofiller preferentially dispersed at the interface (adapted from Ref. [137]).

The precise localization of nanofillers is critical to their compatibilizing effect in polymer and biopolymer blends. Morphology refinement arises through two main mechanisms depending on nanoparticle positioning. When selectively incorporated into one biopolymer phase, the nanofillers also retard relaxation dynamics, preserving finer structures [118,119,98]. Especially when they are segregated into the continuous phase, the nanofiller can form a percolating network that increases viscosity and kinetically traps finely dispersed domains, preventing coarsening (Fig. 8a).

Alternatively, when localized at the interface between immiscible biopolymer phases, nanoparticles can promote finer morphologies and suppress coalescence through steric hindrance effects. Their high surface area and ability to cover the interface provide coupling interactions between the biopolymers, even without strong specific affinity of the nanofiller for both phases. Moreover, rigid plate-like nanoparticles (e.g. nanoclays, graphene) at the interface can frustrate shape relaxation of deformed droplets, enabling stabilization of irregular non-spherical domains. Such irregular morphologies improve blend properties (Fig. 8b) [142].

Both routes highlight how selective nanoparticle-polymer interactions govern the microstructural evolution, stabilizing refined morphologies and enhancing compatibility in nanocomposite blends [137].

The localization of nanofillers in polymer blends depends strongly on the interactions between filler-polymer, filler-filler, and polymer-polymer. Nanofiller geometry also plays a key role - high aspect ratio particles like nanotubes disperse poorly at interfaces compared to low aspect ratio spherical nanoparticles [143]. The underlying mechanism, depending on the different driving forces between the two polymers at the interface in the case of low and high-aspect ratio nanofillers, is represented in Fig. 9 and explained by Yang et al. [101] for the specific case of CNT-induced compatibilization for different couples of polymers and biopolymers.

Thermodynamic factors govern the distribution at equilibrium, while kinetics like blend viscosity, shear rate, and mixing time affect migration rates [144]. Classical wetting theory [145–147] provides a framework for predicting nanofiller localization from interfacial energies between the components. The wetting coefficient ω_a indicates whether a particle will selectively locate in

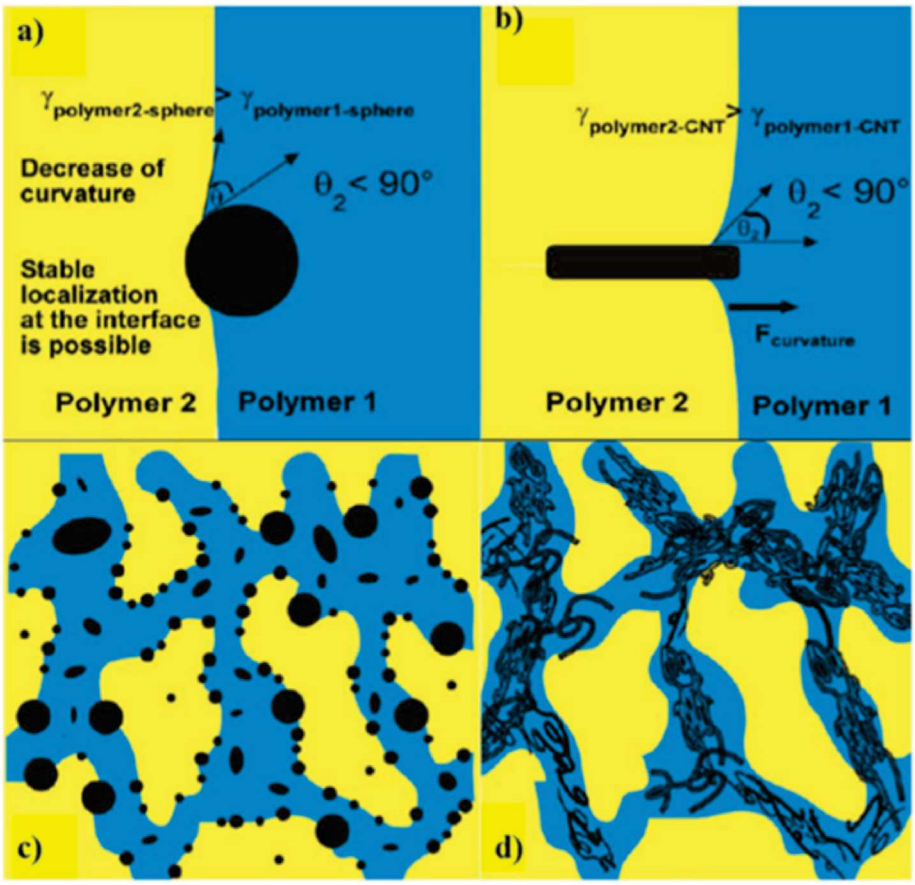

Fig. 9. Low aspect ratio spherical particles (a,c) like carbon black accumulate at interfaces, as the driving force for particle transfer decreases as the nanoparticle crosses the interface, trapping it in the interfacial region. High aspect ratio nanotubes (b,d) experience no such energy barrier during transfer between phases, and therefore they distribute across phases. Tailoring nanoparticle shape and surface properties is key to promoting interfacial segregation for effective compatibilization. (duplicated with permission from Ref. [101]).

polymer phase A, B, or at the A-B interface, as reported in Equation (4):

$$\omega_a = \frac{\gamma_{1/F} - \gamma_{2/F}}{\gamma_{12}} \tag{4}$$

where $\gamma_{1/F}$ is the interfacial energy between polymer 1 and filler F, $\gamma_{2/F}$ is the interfacial energy between polymer 2 and filler, and γ_{12} is the interfacial energy between the two polymer phases. The filler will be preferentially located in polymer 2 when $\omega_a > 1$, in the polymer 1 when $\omega_a < -1$, and at the interface when $-1 < \omega_a < 1$ [136,148,149]. The interfacial energy can be calculated from the surface energies as well as the dispersed and polar components using either the harmonic mean (Equation (5)) in the case of low-energy materials, or the geometric mean in the case of high-energy materials (Equation (6)):

$$\gamma_{12} = \gamma_1 + \gamma_2 - 4\left(\frac{\gamma_1^d \gamma_2^d}{\gamma_1^d + \gamma_2^d} + \frac{\gamma_1^p \gamma_2^p}{\gamma_1^p + \gamma_2^p}\right) \tag{5}$$

$$\gamma_{12} = \gamma_1 + \gamma_2 - 2\left(\sqrt{\gamma_1^d \gamma_2^d} + \sqrt{\gamma_1^p \gamma_2^p}\right) \tag{6}$$

where γ_1 and γ_2 are the surface tensions of phase 1 and phase 2, γ_1^d and γ_2^d are the dispersive components of the surface tensions, and γ_1^p and γ_2^p the polar components [136].

However, challenges remain in applying idealized thermodynamic concepts to complex ternary nanocomposite blends. The relationships between processing conditions, nanofiller properties, and resulting morphology require further study through combined modeling and experimental efforts. Overall, preferential localization of nanoparticles enables compatibilization but depends on many system variables. A detailed understanding of nanofiller distribution and migration is critical for consistent morphology control and property enhancement in immiscible polymer blends.

Many are the examples in the literature of nanofiller-induced compatibilization for biopolymers. For instance, Wang et al. [86] reported using vinyl functionalized graphene (VGN) as a highly effective compatibilizer to enhance the properties of immiscible PLA/PCL blends. The VGN nanosheets react with both PLA and PCL chains during melt mixing in the presence of dicumyl peroxide (DCP), leading to strong interfacial interactions. The reactive compatibilization helped increase the compatibilization effect induced by the nanofiller and further refined the microstructure (Fig. 10), while Fig. 11 illustrates the proposed compatibilization mechanism: DCP generates macroradicals on PLA/PCL chains that react with the vinyl groups on VGN, compatibilizing the blend. The VGN localization and interfacial interactions significantly influenced the blend morphology and properties. The phase size of the co-continuous morphology reduced markedly in reactive blends, indicating enhanced compatibility. Quantitatively, the reactive blend with 2 wt% VGN showed a storage modulus of 3500 MPa at −60 °C, over 200% higher than 1400 MPa for the uncompatibilized blend. The tensile strength

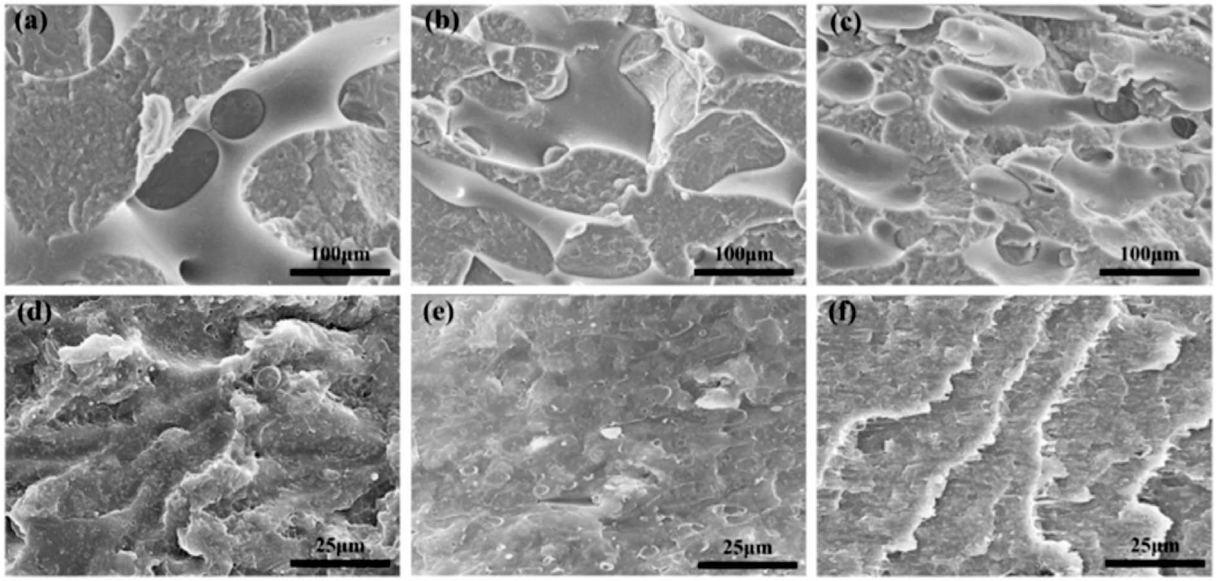

Fig. 10. SEM micrographs of cryofractured surfaces of (a–c) uncompatibilized and (d–f) reactively compatibilized PLA/PCL/VGN blend nanocomposites. Content of VGN: (a, d) 0.5, (b, e) 1.0, and (c, f) 2.0 wt%. Duplicated from Ref. [86].

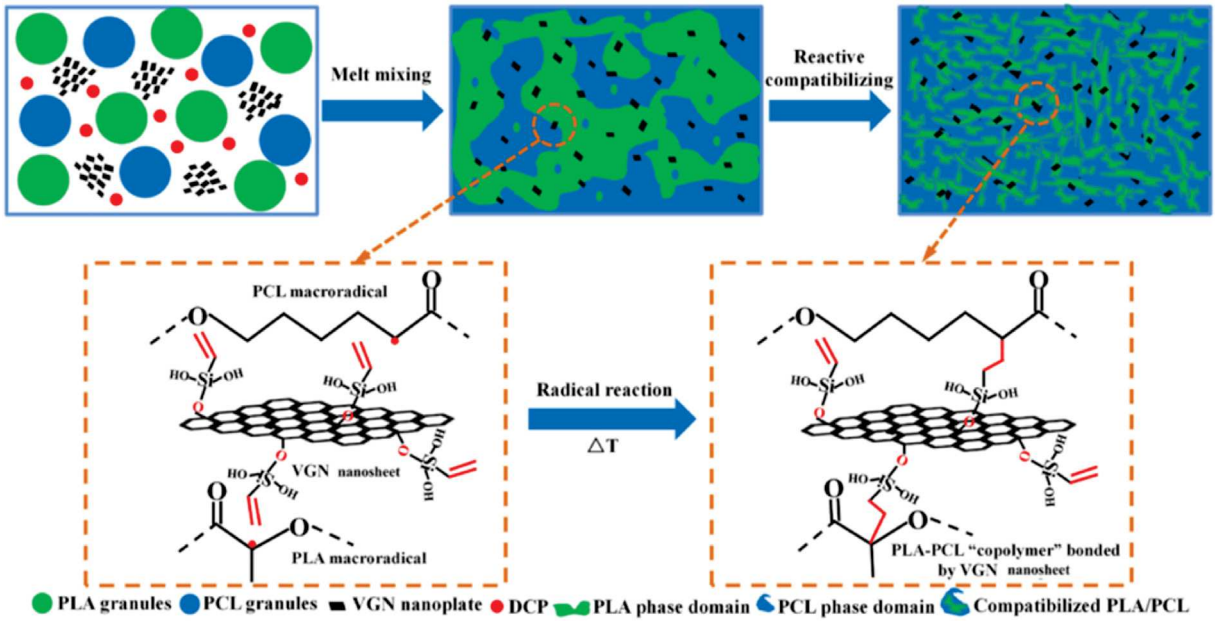

Fig. 11. Schematics of compatibilizing PLA/PCL blend using reactive graphene (VGN) with the aid of DCP during melt mixing. Duplicated with permission from Ref. [86].

increased from 9.1 MPa for the uncompatibilized blend to 32–34 MPa for reactive blends, a ~300% improvement. This is attributed to strong VGN-polymer interfacial interactions. Localization of VGN at the interface thus enables efficient compatibilization and reinforcement.

In another work, Nofar et al. [150] investigated the effects of nanoclay (Cloisite® 30B) content and localization on the morphology and properties of PLA/PBAT blends. Three mixing strategies were used: (1) direct blending, (2) pre-mixing clay with PLA then adding PBAT, and (3) pre-mixing clay with PBAT then adding PLA.

Applying the approach reported in Equation (3), the calculated wetting coefficient ω_a was mostly comprised between −1 and 1, indicating preferential interfacial localization and, in this way, the nanoclay could act as a droplet coalescence barrier. This was confirmed by TEM images showing clay at the interface for 1 wt% loading, irrespective of the mixing approach. The PBAT domain size was reduced from 1.30 μm (neat blend) to 0.70–0.85 μm. On the other hand, with 5 wt% clay (Fig. 12), the mixing route strongly influenced localization. Approach (1) gave interfacial and PLA-clay localization, with 0.65 μm domains. In route (2), clay remained mostly in PLA giving 0.75 μm domains. Route (3) with mixing nanoclay (C30B) first with PBAT showed complete relocation to the interface, providing the finest 0.35 μm domains.

Localization also governed blend stabilization during shearing. The 1 wt% clay blends showed no coalescence, with clay retaining an interfacial position. However, the high interfacial clay in route

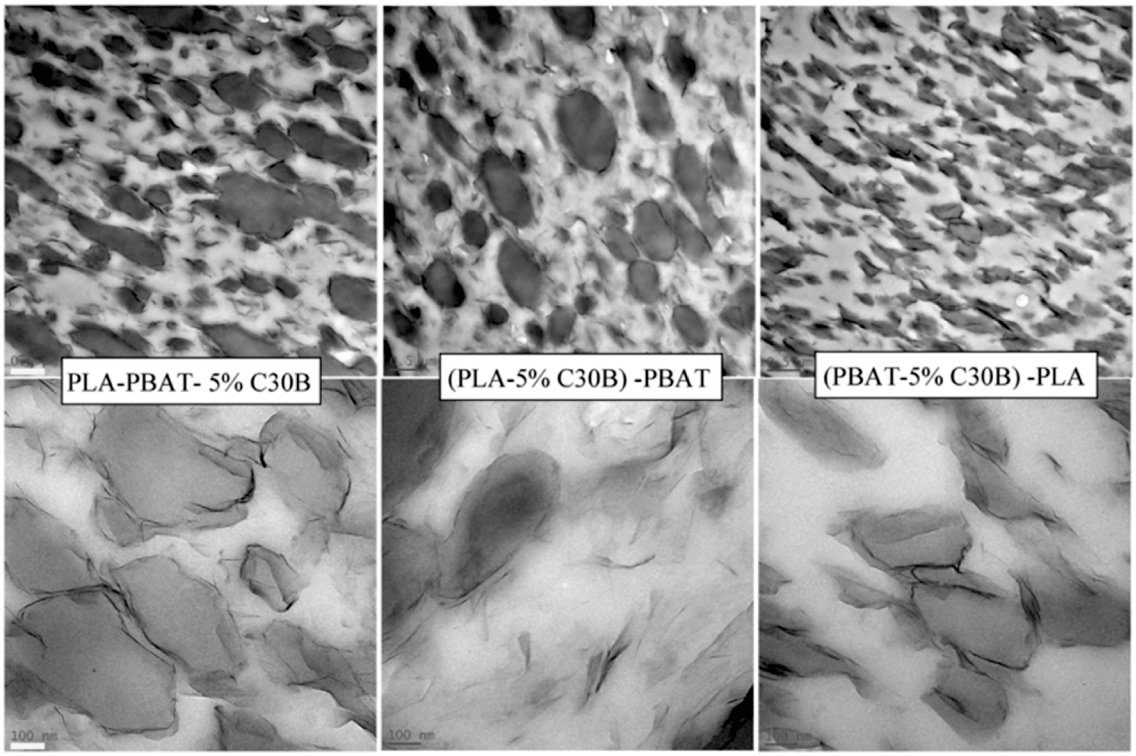

Fig. 12. TEM images showing the PBAT dispersed phase and localization of 5 wt% nanoclay (C30B) within the blend when prepared via the three different strategies. The scale bars for the top and bottom images are 500 and 100 nm, respectively. Duplicated with permission from Ref. [150].

(3) with 5 wt% migrated into PLA during shearing, enabling coalescence. Overall, the results demonstrated clay localization could be tailored via a mixing approach to stabilize blends. Interfacial localization provided the optimal compatibilization and anti-coalescence effects. The findings provided guidance on the design of nanofilled polymer blends with controlled morphology.

5. Evaluation of miscibility and the compatibilization performance

Polymer blending offers a versatile route to develop advanced materials by combining the strengths of different polymers. However, most polymer pairs are intrinsically immiscible due to poor enthalpy of mixing, resulting in phase-separated morphologies and compromised properties. Compatibilization techniques are thus critical to promote miscibility and interfacial adhesion between blend constituents. Thorough characterization is essential to evaluate compatibilization efficacy and guide further optimization.

The ultimate assessment of successful compatibilization involves testing the specific property it aims to improve, such as ductility, toughness, or impact strength. However, supporting techniques like microscopy, rheology, and thermal analysis can provide invaluable insights into the mechanisms and progression of compatibilization. Electron microscopy methods visualize phase morphology and adhesion at the key microstructural level. Rheology probes molecular interactions and dynamics. Thermal analysis detects changes in transition temperatures and crystallization behavior related to miscibility.

This chapter reviews the application of these techniques to compatibilized polymer blends. It emphasizes using property testing in conjunction with microscopy, rheology, and thermal analysis to elucidate structure-property relationships. This multifaceted approach is necessary to comprehensively evaluate compatibilization strategies and determine if the targeted enhancements are achieved. The goal is to establish guidelines for characterizing and optimizing blend miscibility, morphology, interactions, and properties to meet performance objectives. Both experimental results and theoretical modeling provide useful insights into successful blend design.

5.1. Rheological tests

Studying the rheological behavior of polymer blends is of paramount importance for at least two reasons. The first is that when a compatibilizer is added in the melt state, as is generally done industrially, it will unavoidably alter the rheological behavior of the blend. And since it is well known that the viscoelastic and rheological response of the mixture during blending profoundly impacts the optimal processing parameters, the phase morphology formation, and the resulting macroscopic properties, it is clear that investigating the effect of the compatibilizer on the rheological properties is crucial [85].

The second reason why blend rheology is interesting is that it can be useful to quantify the efficiency of compatibilization strategies. However, although many references in the literature deal with the first reason and try to investigate and predict the blend's rheological properties to optimize the processing parameters, very few papers make an effective use of rheology to assess the success of the employed compatibilization strategy. Rheological tests are often neglected in favor of the study of morphology and mechanical properties, which stems largely from the inherent challenges in predicting macroscopic blend properties and performance from rheological measurements and correlations alone, but it is undoubted that rheology can be a valid ally in the preliminary assessment of a compatibilization technique, as well as in optimizing processing protocols and tailored blend design.

The dependence of melt viscosity on composition is generally modeled with the log-additivity rule, which states that the logarithm of the complex shear viscosity of the blend is given by the linear combination of the logarithms of the viscosities of the blend components weighed by their volume fractions. The real viscosity of a heterogeneous polymeric mixture can display either negative or positive deviations from this simple rule: increased blend viscosity relative to model predictions generally indicates enhanced interfacial interactions, a pre-requisite for good blend compatibility, while a decrease points to poor adhesion between phases [19,151].

However, the viscosity and rheological behavior of biopolymer blends may depend on numerous other factors besides compatibilization, including plasticizer weight fraction, the presence of nanofillers, changes in molar mass due to polymerization, reactive compatibilization, or degradation caused by the compatibilizer or residual humidity, and even the order in which the components are mixed.

For example, Al Itry et al. [152] investigated the impact of a multifunctional epoxide (Joncryl®ADR-4368) on the interfacial properties of PLA/PBAT blends via the measurement of their rheological, morphological, and interfacial properties. Rheological measurements revealed significant differences between the uncompatibilized and Joncryl-compatibilized PLA/PBAT blends. The compatibilized blends displayed more shear thinning at all frequencies studied, indicating reactions occurring at the interface between the phases (Fig. 13a).

Examining the storage modulus dependence on frequency gave further insights (Fig. 13b). All blends converged to the same plateau modulus at high frequencies, evidencing similar chain entanglement. However, at lower frequencies, the uncompatibilized PLA/PBAT blend had a higher storage modulus than the pure components, attributed to some interfacial interactions. The Joncryl-compatibilized blends exhibited a further rise in storage modulus at low frequencies due to the formation of higher molecular weight copolymer chains at the interface.

Analysis of Cole-Cole plots (Fig. 13c and d), relating the viscous and elastic moduli, showed the uncompatibilized blend had two relaxations corresponding to the PLA matrix and PBAT phases. In contrast, the compatibilized blends displayed significantly longer relaxation times, reflecting the chain-extending action of the Joncryl reactive modifier. Calculation of weighted relaxation spectra enabled deconvoluting the different relaxation modes. The uncompatibilized blend exhibited three relaxations - from the PLA matrix, PBAT phase, and a longer mode ascribed to the PLA-PBAT transesterification copolymer. The compatibilized blends showed comparable PLA and PBAT relaxations but a far longer relaxation attributed to interfacial PLA-Joncryl-PBAT copolymer relaxation.

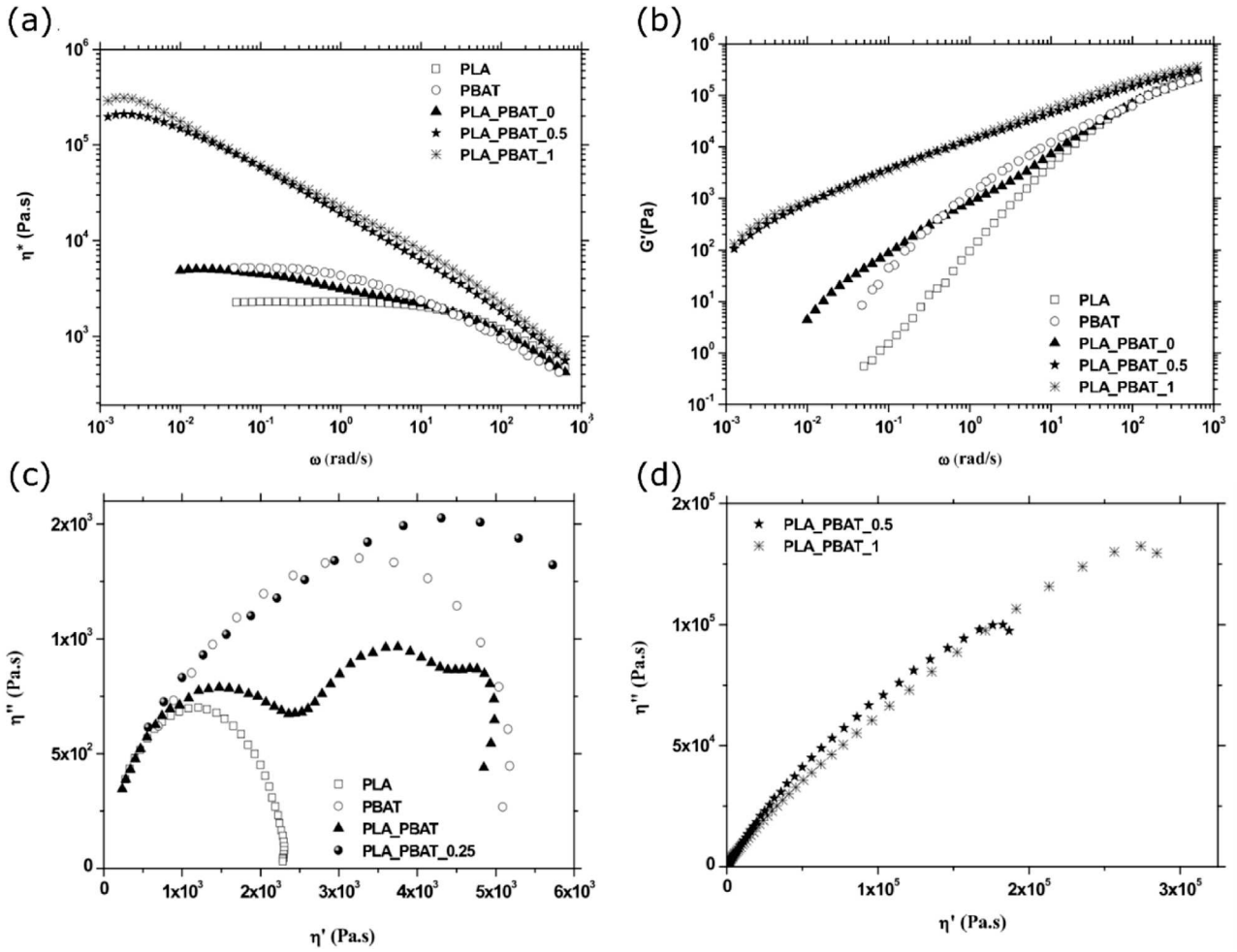

Fig. 13. Rheological investigation (plate-plate dynamic rheometry) of the compatibilization performance of PLA/PBAT/Joncryl blends. The numbers in the legend represent the amount of Joncryl. (a–b) complex viscosity and shear storage modulus at 180 °C as a function of the applied angular frequency; (c–d) Cole-Cole plots at 180 °C. Duplicated with permission from Ref [152].

More recently, Fredi et al. [153] examined the effect of the same epoxy-functionalized compatibilized/chain extender Joncryl (J) on the rheological properties of polylactic acid (PLA) (Fig. 14). Adding J substantially increased the complex viscosity, storage modulus, and loss modulus of neat PLA, with a two-order-of-magnitude increase at 1 ph J loading. This demonstrates J's effectiveness as a chain extender for PLA, counteracting molecular weight loss during high-temperature processing. Neat PLA showed typical linear polymer behavior with rapid chain relaxation. In contrast, PLA-J blends evidenced reduced frequency sensitivity, marked shear thinning, and enhanced melt elasticity from the increased chain entanglement due to J's multifunctionality enabling long-chain branched structures. This highlights the impact that compatibilizers/chain extenders may have in modifying the rheological behavior of polymers and blends regardless of the compatibilization performance and stresses the importance of coupling rheological

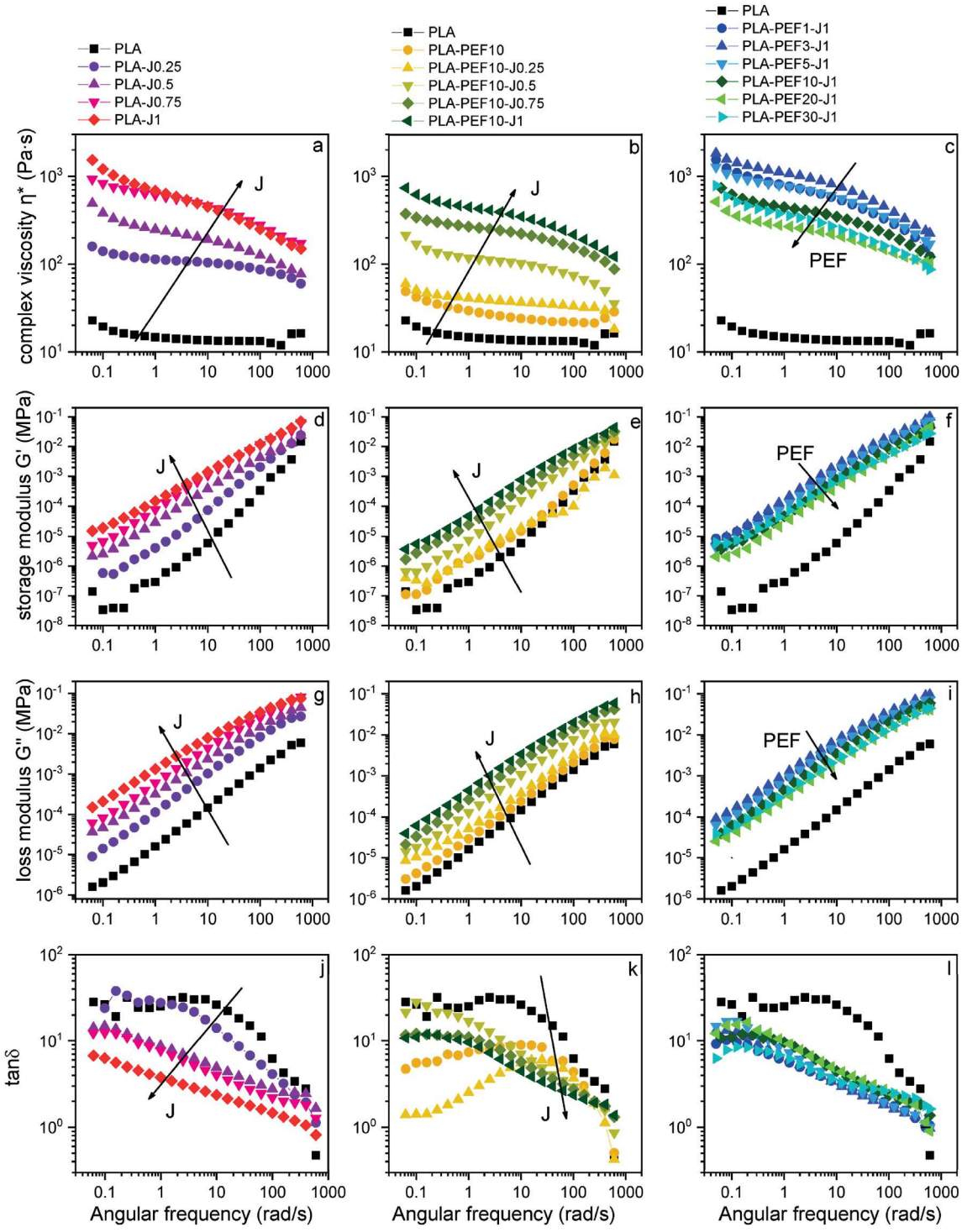

Fig. 14. Results of the dynamic rheological tests at 230 °C on PLA/PEF blends compatibilized with Joncryl (J). Complex viscosity (a–c), storage modulus (d–f), loss modulus (g–i), and tanδ (j–l) as a function of the applied frequency for three series of samples. Duplicated with permission from Ref. [153].

characterization with other tests, to have a more comprehensive overview of the effects of the compatibilizer.

Incorporating 10 wt% poly(ethylene furandicarboxylate) PEF into PLA increased the complex viscosity and moduli, especially at low frequencies. This arose from PEF droplet-PLA interfacial interactions, indicating some compatibility between the polymers. Adding J further enhanced this effect, implying improved interfacial interaction between the PLA and PEF phases due to J's compatibilizing action. However, at a fixed J loading of 1 phr, increasing the PEF fraction appeared to make the compatibilization by J less effective, as shown by decreasing viscosity and moduli with higher PEF content. This suggests the extent of compatibilization depends on the relative amounts of the minor PEF phase and interfacial modifier J.

In summary, the epoxy-functionalized chain extender Joncryl was shown to be highly effective for increasing PLA's molecular weight and melt elasticity through reactive chain extension. Joncryl also enhanced interfacial interactions and compatibility between PLA and PEF, evidenced by rheological changes indicating improved stress transfer between the phases. These results demonstrate how rheological characterization can provide molecular-level insights into compatibilization mechanisms in reactive polymer blends.

5.2. Microstructure and morphology

As discussed in the previous chapters, immiscible polymer blends generally show a sea-island microstructure, with the minoritarian component present in the form of dispersed particles, the size and distribution of which are the result of a competitive process between breakup and coalescence phenomena. The degree of dispersion is determined by interfacial interactions, the viscosity ratio of the blend components, but also by processing parameters such as the shear rate of mixing [62].

The ideal, targeted microstructure is generally a finely dispersed second phase showing a strong interfacial adhesion with the majoritarian component. Such a microstructure leads to improved physical-mechanical properties and is therefore associated with a successful compatibilization strategy, given the aforementioned definition of compatibility. These improvements can stem from greater interfacial interactions and/or larger interfacial surface area due to morphological modifications. However, it should be noted that the aim of compatibilization is not to make immiscible blends fully miscible. Rather, the goal is to suitably control blend morphology and strengthen interfacial adhesion to tailor mechanical performance as needed [107,124].

In most blend systems, the major component forms the continuous phase while the minor component forms the dispersed phase. However, phase inversion can occur at certain compositions where the phases switch roles. This happens when the polymers are present in roughly equal amounts or at high loadings of the minor phase. Various morphologies can be generated through melt mixing, including spherical, lamellar, fibrillar, and even co-continuous structures. Co-continuous morphologies feature interpenetrating networks of both phases. This structure is particularly advantageous since both components can fully contribute to the blend's properties, leading to synergistic improvements [19].

For example, Mazidi et al. [113] used poly(methyl methacrylate) (PMMA) as a compatibilizer for PLA/polycarbonate (PC) blends with improved toughness, as PLA has been proven to be partially miscible with both PLA and PC. Interfacial energy calculations predicted PMMA would localize at the PLA/PC interface due to its miscibility with both components. Dynamic mechanical analysis confirmed PMMA promoted molecular mixing of PLA and PC chains across phase boundaries. In PLA/PC/PMMA blends, SEM showed finer, more homogeneous PC dispersion and improved interfacial adhesion versus uncompatibilized PLA/PC, evidencing PMMA's compatibilization effect. Transmission electron microscopy (TEM) revealed a partial wetting stack-like morphology, with PMMA concentrated around PC domains (Fig. 15). Mechanical testing demonstrated significantly enhanced tensile and flexural ductility for compatibilized versus neat PLA/PC blends, while maintaining stiffness, attributed to more effective stress transfer enabled by the improved phase morphology and adhesion. However, impact strength remained limited.

To further toughen the PLA/PC/PMMA blend, the authors added core-shell polybutadiene-*graft*-poly(styrene-*co*-acrylonitrile) (PB-*g*-SAN) particles. The PB-g-SAN shell interacted with PC and PMMA phases but not PLA. SEM and TEM showed PB-g-SAN produced even finer, more homogeneous dispersion of PC/PMMA domains, developing an interconnected co-continuous morphology with PB-g-SAN concentrated around domains (Figs. 16 and 17). Dynamic mechanical analysis revealed decreasing miscibility between PMMA-rich and PLA-rich regions with more PB-g-SAN, as SAN displaced PMMA chains. This interconnected morphology enabled massive plastic deformation under impact observed in SEM, giving exceptionally high toughness. A 690 J/m impact strength was achieved with 24 wt% PB-g-SAN, a 28× increase versus neat PLA.

In summary, microstructure characterization at multiple length scales was crucial for understanding and optimizing the compatibilization strategies. Interfacial energy calculations, electron microscopy, and dynamic mechanical analysis provided critical insights into phase interactions, miscibility, dispersion, adhesion, and morphology. This elucidated the compatibilizers' effects on structure-property relationships, guiding blend optimization to achieve the desired mechanical performance, especially the targeted balance of stiffness, ductility, and impact toughness.

Microstructural characterization can be also useful to assess the degree of interaction and its possible improvement through compatibilization quantitatively. In fact, the Flory–Huggins interaction parameter (χ_{12}) can be related to the size of the dispersed particles (r), as described in Equations (7) and (8) [154]:

$$r = \frac{4\alpha\gamma_{12} f(\eta_{rel})}{\pi\eta_m}\varphi_d \tag{7}$$

$$\gamma_{12} = \frac{bRT\sqrt{\chi_{12}}}{V_r} \tag{8}$$

where α is the coalescence probability of particles, γ_{12} the interfacial tension, $f(\eta_{rel})$ a function of the relative viscosity of the components, η_m the matrix viscosity, φ_d the volume fraction of the dispersed phase, b is the effective monomer length, and V_r the molar reference volume. χ_{12} can also be correlated with the thickness of the interphase (l) [20,62,154], as reported in Equation (8):

$$l = \frac{b}{\sqrt{\chi_{12}}} \tag{8}$$

5.3. Mechanical characterization

The impact of compatibilization is frequently described based on morphological examinations, without addressing mechanical performance. This may, however, be insufficient since enhancing mechanical properties is often the primary goal of modification techniques [20,62]. Another common claim is that improved compatibility is shown by an increased Young's modulus. However, compatibilization most often aims to improve interfacial adhesion

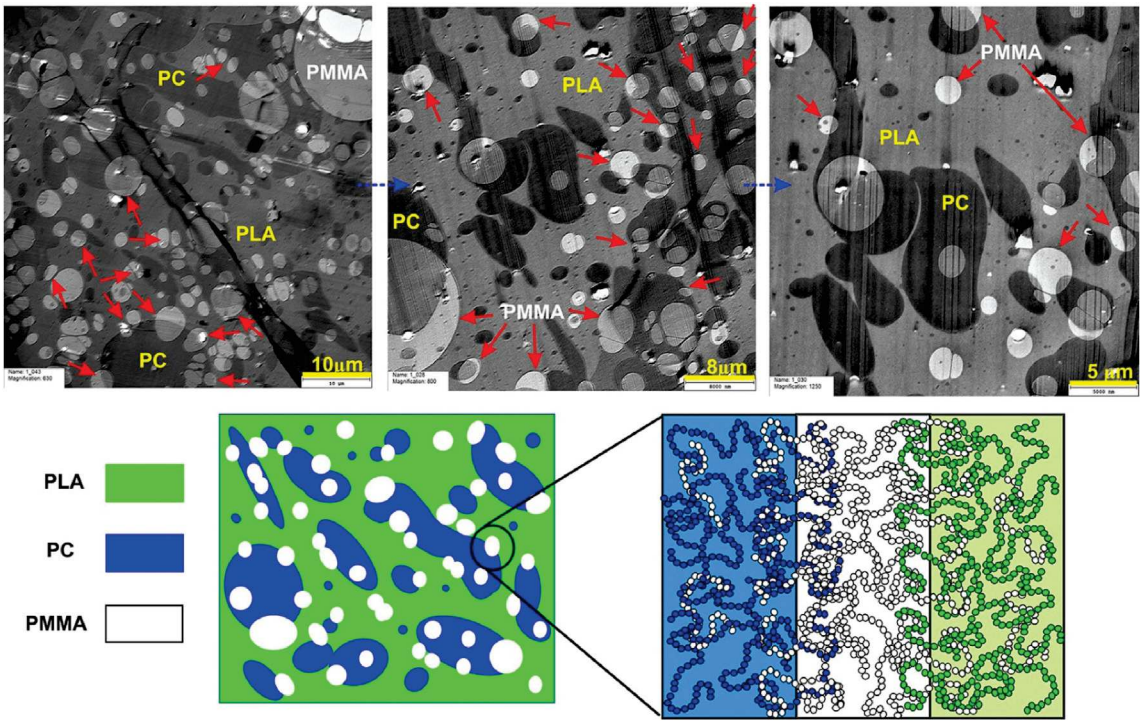

Fig. 15. TEM micrographs of the ternary blend PLA/PC/PMMA (40/40/20 wt/wt/wt) at different magnifications and schematic representation of the morphology developed in the blend, showing the partial miscibility of the components. Duplicated with permission from Ref. [113].

between components, and the elastic modulus relates to behavior at very low deformations, under which conditions the interfacial phase separation is often negligible [154]. Thus, stiffness alone does not adequately indicate interfacial adhesion strength. Although compatibilization alters the composition and often causes structural changes like reduced dispersed phase size, thereby influencing the stiffness, this correlation is rarely direct and rather complex, since side reactions, plasticization, or crystallization from adding a compatibilizer also have similar effects. Consequently, blend or composite modulus is not an appropriate indicator of compatibility on its own [62,154].

On the other hand, a common result of effective compatibilization is increased tensile strength or the strain at break of the blend, thereby leading many researchers to observe the trend of these properties when evaluating various compatibilization approaches [92,75,88,142,155,156]. In fact, by promoting interdiffusion and interactions between phases, compatibilization enhances interfacial adhesion, and this allows applied stresses to be transferred more efficiently across phase boundaries without debonding and premature crack initiation. Also, the finer dispersion of the minor phase and morphology modifications like co-continuity, often induced by compatibilization, bolster mechanical performance by requiring cracks to traverse more interfaces and engage larger volumes in deformation [70,79,97]. Additionally, compatibilization facilitates cooperative motions and plastic flow of phases due to increased molecular mixing, which allows advantageous properties of each component, like ductility and strength, to work synergistically when stresses are applied. Finally, compatibilization may also induce advantageous crystallization or other structural changes in a phase that augment its mechanical response.

Nonetheless, assessing compatibilization efficacy solely based on mechanical characteristics is not always sufficient. While tensile strength is practically important, this single value does not reveal the reasons for the success or failure of a given compatibilization method. To tailor the properties of biopolymer blends, a detailed analysis of chemical structure, morphology, and mechanical behavior including micromechanical deformation processes is needed. This allows for the identification of the key mechanisms under the property enhancements and the factors that still limit the performance.

For example, Avci et al. [114] investigated the effects of an internal lubricant and MA on the properties of PLA/TPU blends. Mechanical testing showed the TPU elastomer lowered the tensile and flexural strength of PLA by 40–50% but significantly enhanced the strain at break. This stems from the soft TPU segments increasing chain mobility. While reducing stiffness and strength, the lubricant further improved tensile and flexural elongation by 15–20% due to its plasticizing effect. In contrast, MA compatibilization increased elongation by 60% along with tensile and flexural strength compared to plain PLA/TPU, attributed to stronger interfacial adhesion enabling more efficient stress transfer. Fig. 18 presents the key mechanical test results, showing an increased ductility for the blends compared to neat PLA. The PLA/TPU blend had an impact strength of 46.0 kJ/m^2, over 3 times higher than PLA's 15.9 kJ/m^2. With MA, impact strength reached 52.8 kJ/m^2 due to enhanced phase compatibility. However, the lubricant decreased impact strength to 39.2 kJ/m^2, likely because of weaker interaction with MA reducing its effectiveness. Overall, the study demonstrated that proper TPU and MA addition substantially increased PLA's strain at break, impact resistance, and energy absorption during mechanical deformation. This improves ductility and toughness, making PLA more suitable for engineering applications requiring these attributes.

In another study, Zhu et al. [102] investigated PCL/PLA blend (70/30 wt/wt) containing carbon CNTs and organically-modified montmorillonite (MMT) as compatibilizers, for applications as tissue engineering scaffolds such as fixation of facial fractures and

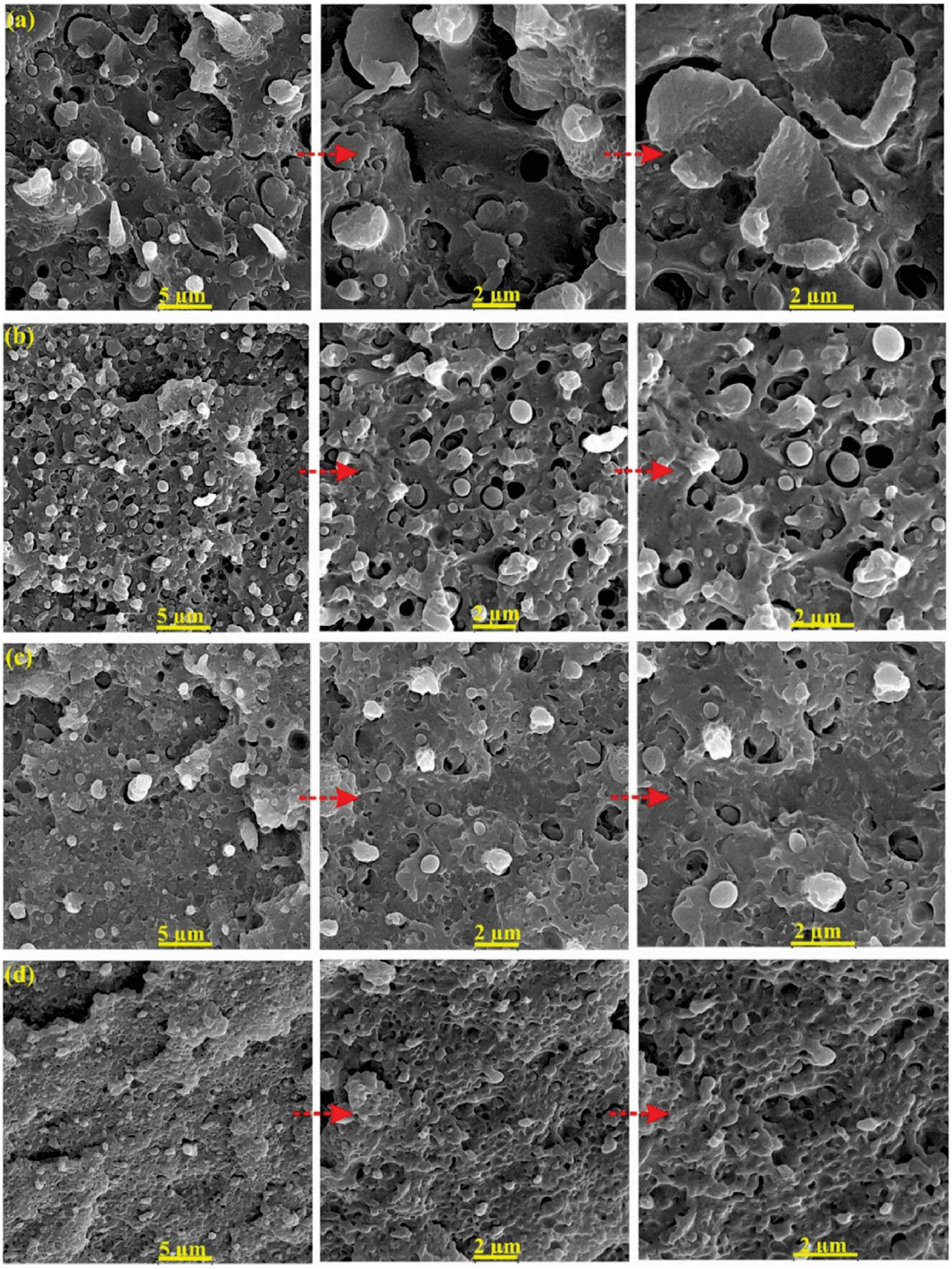

Fig. 16. SEM micrographs of cryofractured surfaces of the PLA/PC/PMMA (40/40/20 wt/wt/wt) blend containing various amounts of PB-g-SAN impact modifier: (a) 6 wt%, (b) 12 wt%, (c) 18 wt%, and (d) 24 wt%. Duplicated with permission from Ref. [113].

chemotherapeutic implants. The blends contained 0.5–1 wt% of CNTs and/or MMT. TEM confirmed the selective distribution and revealed a finer, more uniform PLA droplet size with nanofillers versus neat PCL/PLA. More specifically, CNTs were localized in the PCL phase, forming a network structure, while MMTs were located at the interface between the PCL and PLA domains.

Fig. 19 shows mechanical testing results. While lowering modulus slightly, CNTs or MMT alone increased elongation at break and tensile strength significantly, attributed to the percolated CNT network reinforcing PCL and MMT enhancing interfacial adhesion. However, the CNT/MMT combination had the best performance, giving 137% and 80% improvements in strain at break and strength, respectively, versus neat PCL/PLA. A synergistic toughening effect was demonstrated, ascribed to the co-localized CNT network and MMT interfacial interaction.

SEM micrographs of the fractured tensile specimens in Fig. 20 provided further evidence. Neat PCL/PLA showed a clear two-phase sea-island morphology indicating poor adhesion. With

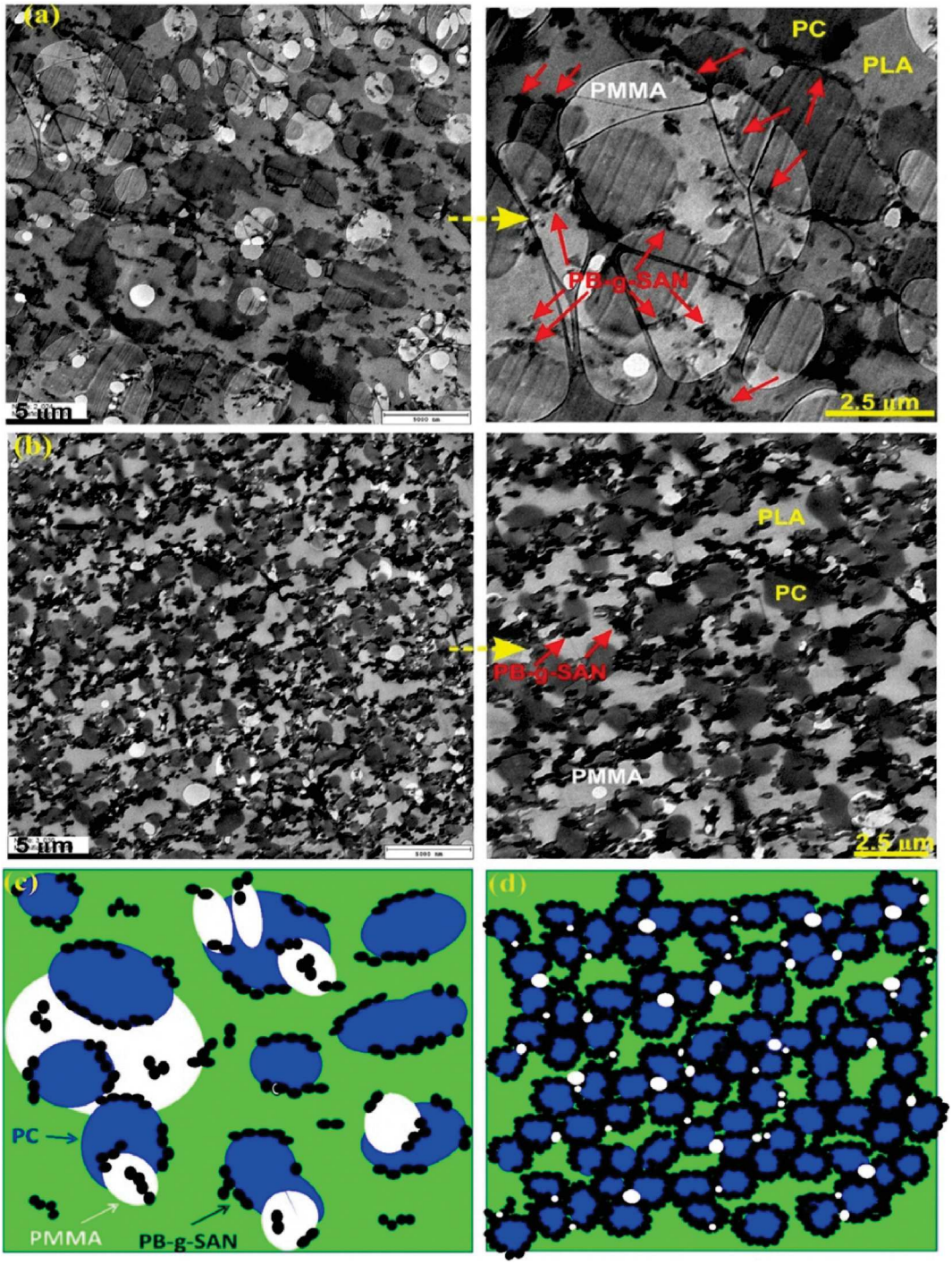

Fig. 17. (a, b) TEM micrographs of PLA/PC/PMMA (40/40/20 wt/wt/wt) blend containing 6 wt% (a) and 24 wt% (b) of PB-g-SAN. (c, d) Schematic drawing of the morphology developed in toughened quaternary blends containing 6% (c) and 24 wt% (d) of PB-g-SAN. Duplicated with permission from Ref. [113].

added CNTs or MMT, more plastic deformation was observed, suggesting enhanced compatibility and adhesion. The CNT/MMT blends displayed the most drawn, fibrous matrix and deformation, consistent with the synergistic toughening mechanism. In summary, a tailored combination of selectively located CNTs and MMT improved PCL/PLA blend morphology, compatibility, and stress transfer efficiency. This produced remarkable simultaneous enhancements in ductility, strength, and modulus that outperformed either nanofiller alone. Microscopy coupled with mechanical and rheological testing was crucial in elucidating the synergistic toughening mechanisms. This nanofiller approach enables the tuning of PCL/PLA blends for specialized applications in areas including tissue engineering.

As mentioned previously, some mechanical properties are more suitable than others to prove that a compatibilization strategy is promising. In fact, if the elastic modulus depends mostly on composition and less on interaction, some other properties like yield stress and tensile strength strongly depend on miscibility and structure and are very sensitive to changes in interactions between the phases [20].

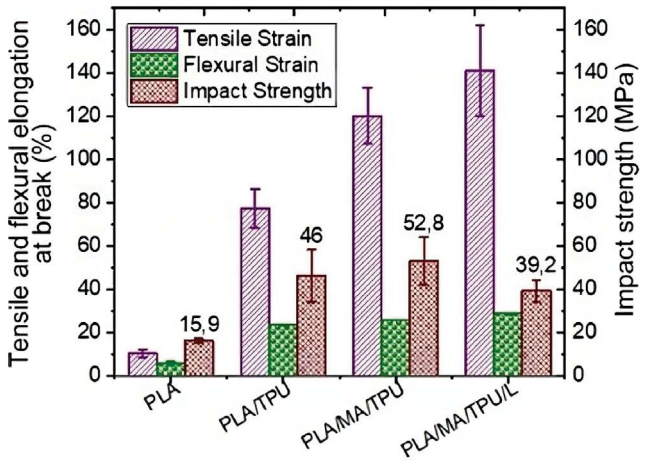

Fig. 18. Tensile and flexural strain at break and impact strength of PLA, PLA/TPU blend, MA-compatibilized PLA/TPU blend, and the MA-compatibilized PLA/TPU blend containing a commercial lubricant. Duplicated from Ref. [114].

More specifically, as described by Fekete et al. [154], the correlations developed to describe the composition dependence of the mechanical properties of particle-filled polymers can be also adapted to polymer blends. The correlation between the volume fraction of the dispersed phase (φ_d) and the yield stress and tensile strength can be expressed through Equations (10) and (11), respectively:

$$\sigma_y = \sigma_{y0}\frac{1-\varphi_d}{1+2.5\varphi_d}\exp\left(B\varphi_d\right) \tag{10}$$

$$\sigma_T = \sigma_{T0}\lambda^n\frac{1-\varphi_d}{1+2.5\varphi_d}\exp\left(B\varphi_d\right) \tag{11}$$

where σ_y and σ_{y0} are the yield stress of the blend and the matrix (the continuous polymer phase), respectively, σ_T and σ_{T0} are the true tensile strength ($\sigma_T = \sigma\lambda; \lambda = L/L_0$) of the blend and the matrix, respectively, n reflects the strain-hardening properties of the matrix, and B reflects the interaction, being proportional to the load carried by the dispersed component. B can be determined from the ratio between the strength of the dispersed phase (σ_{Td}) and that of the continuous phase (σ_{T0}), through Equation (12):

$$B_T = \ln\left(C\frac{\sigma_{Td}}{\sigma_{T0}}\right) \tag{12}$$

where C is related to the interactions, i.e., to the stress transfer between the phases, and inversely correlates to the Flory-Huggins interaction parameter.

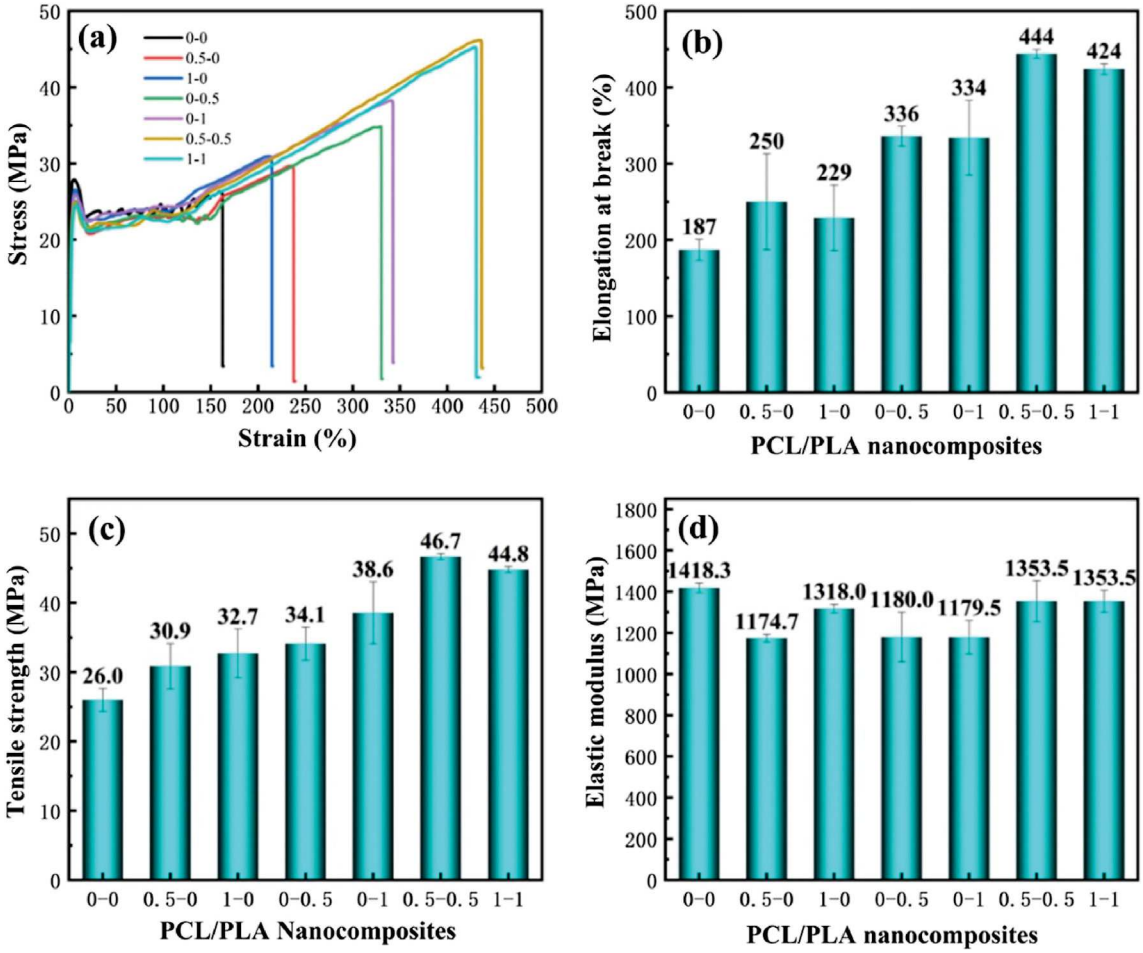

Fig. 19. Mechanical properties of PCL/PLA nanocomposites compatibilized with CNTs and MMT: (a) representative stress-strain curves, (b) strain at break, (c) tensile stress, and (d) elastic modulus. Duplicated with permission from Ref. [102].

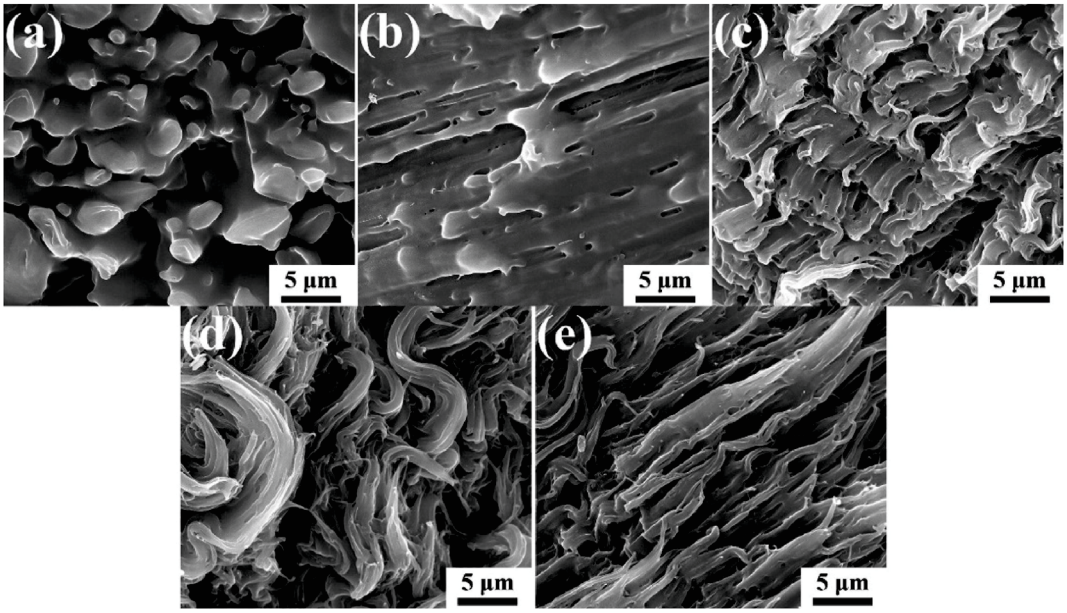

Fig. 20. SEM images of the fracture surface of PCL/PLA nanocomposites after the test: (a) no nanofillers; (b) blend containing 0.5% of CNTs, (c) blend containing 0.5% of MMT, (d) blend containing 0.5% of both nanofillers, and (e) blend containing 1% of both nanofillers. Duplicated with permission from Ref. [102].

5.4. Thermal characterization

Thermal characterization of biopolymer blends with techniques like DSC and DMTA can be a useful tool to investigate the success of a compatibilization route, as they allow measuring the shifts in the relaxation temperatures as a result of the blend miscibility level and compatibilization. For example, DSC and DMTA are commonly used to determine the T_g of blend phases. A single T_g intermediate between the values of the neat components is often taken as an indication of miscibility. However, it is important to note that if the T_g difference between the two parent polymers is not large enough (less than 20–30 °C), most methods cannot detect separate T_g s even for immiscible, heterogeneous blends. Frequently, two distinct T_g s are observed that shift closer together with changing blend ratio. Such results are usually only assessed qualitatively, with good interaction inferred from the T_g trends.

When it is possible to clearly detect the T_g shifts, these results could be analyzed quantitatively, for example by using the approach of Kim and Burns [103]. In this work, the authors have developed a method to quantify miscibility and the Flory-Huggins interaction parameter χ_{12} by measuring the T_g and the specific heat increment ΔC_p at the T_g of the blends. The method is based on the determination of the T_g shifts of the two polymer phases, which is caused by partial miscibility, and on the subsequent calculation of the apparent weight fraction of polymer 1 dissolved in the polymer 2-rich phase and vice versa. The authors start from the empirical equation often used to describe the dependence of T_g on composition in random copolymers and plasticized systems, described in Equation (13):

$$T_g = \omega_1 T_{g1} + \omega_2 T_{g2} \tag{13}$$

where T_g is the observed T_g of the blend or copolymer, ω_1 and ω_2 are the weight fractions of homopolymers 1 and 2, and T_{g1} and T_{g2} the respective T_gs. Therefore, the weight fraction of polymer 1 in the polymer 1-rich phase ω_1' can be written as (Equation (14))

$$\omega_1' = \frac{T_{g1,b} - T_{g2}}{T_{g1} - T_{g2}} \tag{14}$$

where $T_{g1,b}$ is the measured T_g of polymer 1 in the blends. The same can be applied for ω_2'', which is the weight fraction of polymer 2 in the polymer 2-rich phase, once determined $T_{g2,b}$, i.e., the glass transition temperature of polymer 2 in the blends.

Once determined the relative weight fractions in all phases, one can calculate the theoretical T_gs with the Fox or Couchman equations, given by Equations (15) and (16), respectively:

$$\omega_1' = \frac{T_{g1}\left(T_{g1,b} - T_{g2}\right)}{T_{g1,b}\left(T_{g1} - T_{g2}\right)} \tag{15}$$

$$\omega_1' = \frac{\Delta C_{p2}\left(lnT_{g1,b} - lnT_{g2}\right)}{\Delta C_{p1}\left(lnT_{g1} - lnT_{g1,b}\right) + \Delta C_{p2}\left(lnT_{g1,b} - lnT_{g2}\right)} \tag{16}$$

where ΔC_p is the difference in molar heat capacity of the liquid and the solid at T_g.

Another approach is related to the study of miscibility starting from the evaluation of the crystallization behavior and the melting temperatures. A number of studies have examined the crystallization behavior and crystalline structure of biopolymers, sometimes in relation to miscibility. In fact, changes in component melting points can be used to determine interaction strengths based on Flory-Huggins lattice theory, following the method developed by Nishi and Wang [104]. This method works particularly for blends in which one parent polymer is semicrystalline and the other is amorphous and studies the melting point depression of the semicrystalline polymer as a function of the amount of the amorphous one, relating this to miscibility. The Nishi-Wang equation is a well-established way to correlate the melting point depression to the Flory-Huggins interaction parameter χ_{12}, as shown in Equation (17):

$$-\left[\frac{\Delta H^0 V_1}{RV_2}\left(\frac{1}{T_{mb}^0} - \frac{1}{T_m^0}\right) + \frac{ln\,\varphi_2}{N_2} + \left(\frac{1}{N_2} - \frac{1}{N_1}\right)\varphi_1\right] = \beta = \chi_{12}\varphi_1^2 \tag{17}$$

where T^0_{mb} and T^0_m are the equilibrium melting temperatures of the semicrystalline polymer in the blend and in the pure state, respectively, ΔH^0 is the melting enthalpy of the semicrystalline polymer, V_1 and V_2 are the molar volumes of the repeat units in the amorphous and crystalline polymers, respectively, N_1 and N_2 are the degrees of polymerization of the amorphous and semicrystalline polymer, respectively, and φ_1 is the volume fraction of the amorphous polymer in the blend.

This method has been used, for example, by Hou et al. [157], who investigated the polymorphism and enzymatic degradation of poly(1,4-butylene adipate) (PBA) and its binary blends with atactic PHB (aPHB) and poly(vinyl phenol) (PVPh). PBA exhibits polymorphism, forming α and β crystalline forms depending on crystallization temperature. The effects of blending PBA with aPHB and PVPh on the polymorphic behavior and enzymatic degradation rate were studied. The miscibility of the polymer blends was determined using the Nishi and Wang equation, based on the melting point depression of PBA in the blends. The calculated interaction parameters were negative for both blends, indicating that PBA was miscible with both aPHB and PVPh, though the interaction was stronger with PVPh ($\chi_{12} = -1.11$) than with aPHB ($\chi_{12} = -0.27$). Moreover, the crystallization behavior of PBA was affected by blending. Both aPHB and PVPh lowered the critical crystallization temperatures for α and β forms compared to neat PBA. The strong interaction between PBA/PVPh had a greater effect than the weaker PBA/aPHB interaction. Blending also accelerated the β-to-α phase transition of PBA during annealing. The transition occurred at lower temperatures for the blends compared to neat PBA, which was attributed to the decreased melting points. The phase transition was fastest for PBA/PVPh, followed by PBA/aPHB and neat PBA.

More recently, Barbosa et al. [122] investigated the plasticization of PHBV using an oligomeric polyester based on lactic acid, adipic acid, and 1,2-propanediol (PLAP). After DSC tests (Fig. 21) the Flory-Huggins interaction parameter χ_{12} was calculated using the Nishi-Wang equation to determine the miscibility between PHBV and PLAP. The χ_{12} values ranged from −0.299 to −0.081 with PLAP fractions ranging from 10 to 30 wt%, indicating miscibility due to the negative values. However, χ_{12} became less negative at higher PLAP contents, suggesting a critical composition above which phase separation occurred. This critical composition was identified at 37% extrapolating the χ_{12} values to 0.

It was interesting to observe that a similar critical PLAP fraction was identified via DMTA, which revealed multiple relaxations related to rigid and mobile amorphous phases in PHBV. Using the Fox equation, the compositional dependence of the glass transition temperature was used to estimate the PLAP distribution in these phases, and PLAP was preferentially partitioned into the mobile amorphous phase. At 30 wt% PLAP, a PLAP-rich phase formed, indicating incipient phase separation. Hence, the critical PLAP content was estimated as 0.36 from the dynamic mechanical data. This composition data agreed with the observed phase separation.

PLAP also affected the PHBV lamellar structure and spherulitic morphology. Increasing PLAP increased the long period and interlamellar layer thickness up to 0.2 wt% PLAP. Above this, phase separation disrupted the morphology.

The DSC results agreed well with the polarized optical microscopy (POM) images presented in Fig. 22, which provided visual evidence of the phase separation that occurred in the PHBV/PLAP blends at high PLAP concentrations. For PLAP contents at or below 20 wt%, the micrographs showed the typical Maltese cross spherulitic morphology expected for semicrystalline PHBV. The size of these spherulites increased progressively with crystallization temperature, as the degree of supercooling decreased. However, the spherulite size was not substantially impacted by the incorporation of PLAP up to 20 wt%, implying that the blend remained miscible in this composition range.

The situation changed dramatically for the PHBV blend containing 30 wt% PLAP. Throughout the POM images, dark circular spots were visible within the spherulites. These spots indicated the presence of an additional PLAP-rich amorphous phase that arose due to the phase separation of the blend at this high PLAP loading. This phase separated on larger length scales not detectable by small angle X-ray scattering (SAXS), highlighting the value of POM for directly visualizing the morphology. The occurrence of phase

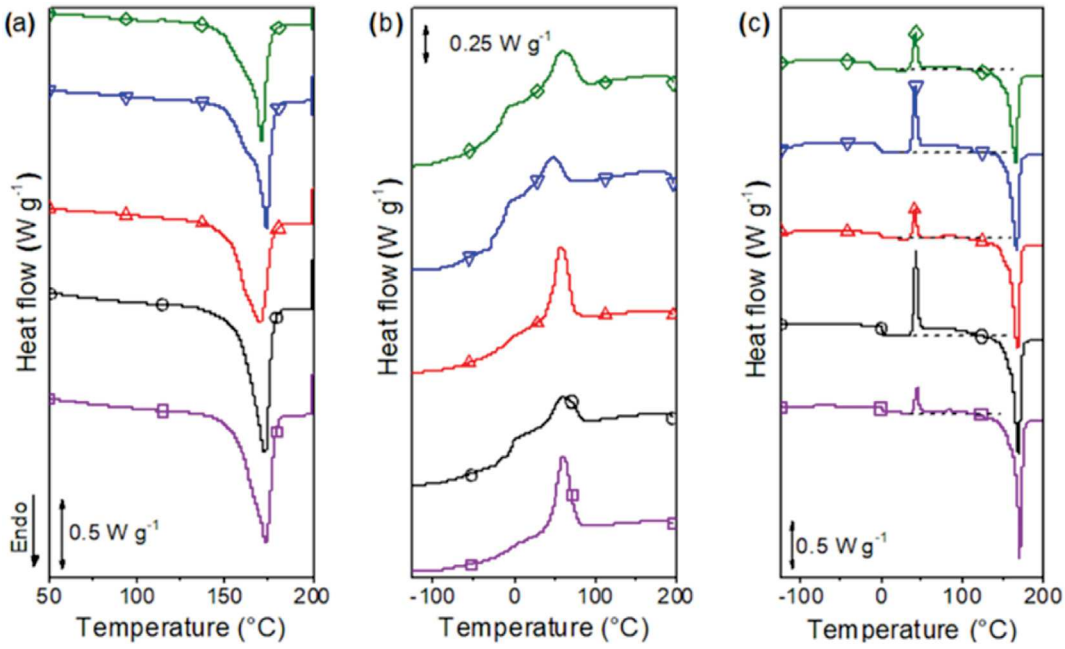

Fig. 21. (a) First heating, (b) cooling, and (c) second heating DSC scans of unprocessed PHBV (□) and processed PHBV (○) and PHBV/PLAP blends with PLAP mass fractions of 10% (red, triangle up open), 20% (blue, open triangle down), and 30% (green, open tilted square). Duplicated with permission from Ref. [122].

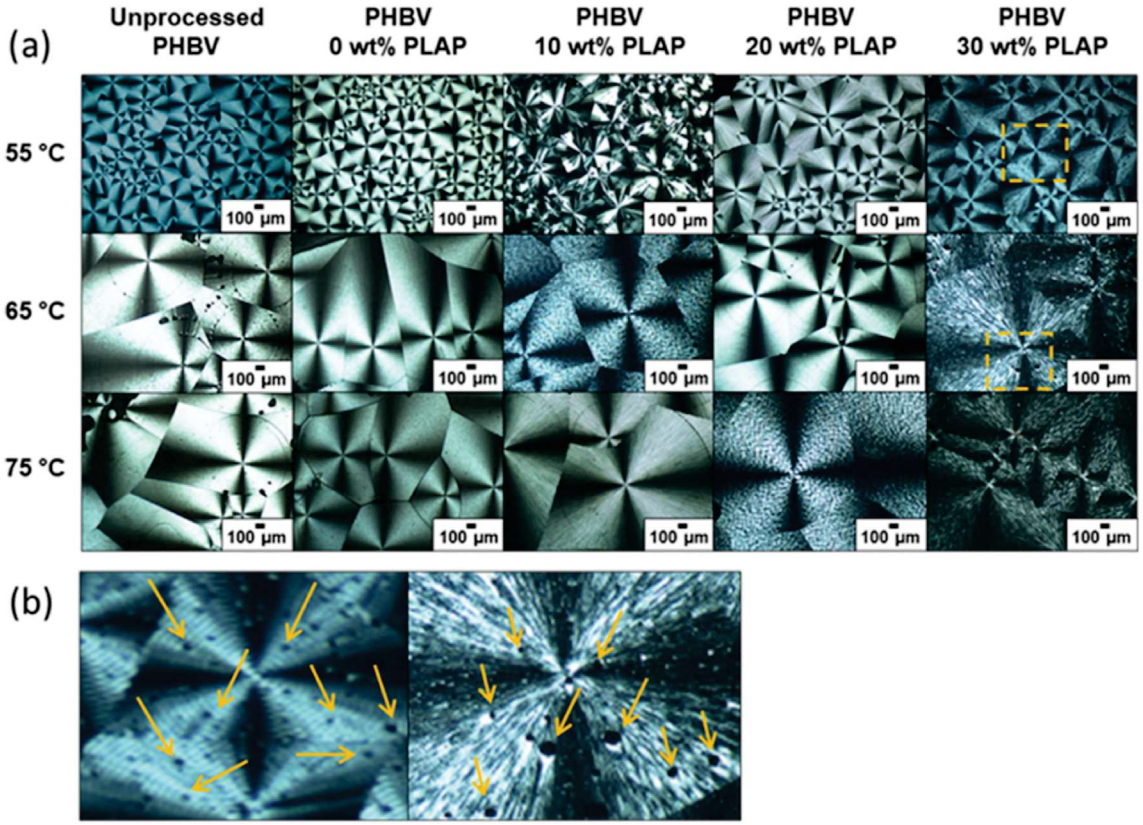

Fig. 22. (a) POM images of unprocessed PHBV, processed PHBV, and its blends with PLAP isothermally crystallized at 55, 65, and 75 °C. (b) High magnification view of the region (highlighted in yellow) of the spherulites in the formulation with wPLAP = 0.30 crystalized at 55 °C (left) and 65 °C (right) with arrows indicating the presence of circular dark spots. Duplicated with permission from Ref. [122].

separation correlated well with the critical PLAP composition between 30 and 36 wt% determined from analysis of the interaction parameter and dynamic mechanical data. Beyond this critical concentration, the typical semicrystalline morphology was disrupted due to PLAP phase separation, leading to poorly defined, irregular spherulites. Thus, the POM images provided a vivid, visual confirmation of the immiscibility and phase separation that set in at high PLAP loadings, consistent with the polymer blend characterization.

6. Biodegradability of biopolymer blends

Since one of the main advantages of biopolymers like PLA, PHAs, and TPS is that they feature biodegradation and/or composting as a possible end-of-life strategy, it is often of remarkable importance to evaluate the biodegradability of the corresponding blends. For example, the functional and environmental advantage of incorporating a non-biodegradable elastomer such as natural rubber as an impact modifier in PLA must overcome the disadvantage of not being able to be composted at the end of its life. From a purely environmental perspective, the balance of such a strategy is not necessarily negative. A rubber-toughened PLA may be more resistant to crazing and fractures, which may prolong the shelf life of the packaged food, and, at the end of its own life, it may be recycled mechanically, chemically, or enzymatically. It is thus fundamental to look at the big picture (i.e., apply rigorous life cycle assessment (LCA) studies) and quantitatively evaluate the overall environmental impact of the selected strategy, remembering that there are no simple answers to complex problems and avoiding falling in vicious and polarized speeches that the discourse over plastics and bioplastics often rises.

In the scientific literature, many research works deal with the microstructural and thermomechanical properties of bioplastic blends, but only a few of them investigate how the blend composition or the adopted compatibilization strategy affects the biodegradation rate. This is important not only when a biodegradable polymer is blended with a non-biodegradable one, but also in the case of blends containing only biodegradable polymers. In fact, the crystallization, polymorphism, and in general the microstructural variations induced by blending and compatibilization may change the biodegradation mechanism and affect the biodegradation rate [157]. For example, the study by Palai et al. [96] investigated the biodegradation behavior of blown films prepared from neat PLA, PLA/PBSA blends, and PLA/TPS blends when buried in soil for 90 days. The results showed that the blend composition significantly affected the biodegradation rate. The PLA/TPS blend exhibited the fastest degradation rate with 40% weight loss in 90 days due to the rapid assimilation of the TPS component by microorganisms in the soil followed by increased degradation of the PLA matrix (Fig. 23). In contrast, the PLA/PBSA blend showed only 8.6% weight loss as it contained 95% PLA whose degradation starts predominantly by abiotic hydrolysis. The neat PLA film degraded the slowest with 5.8% weight loss in 90 days. The hydrophilic nature of TPS in the PLA/TPS blend enhanced moisture absorption from the soil which accelerated hydrolytic degradation of PLA. This priming effect of TPS over PLA can be very useful in the perspective of producing PLA-based soil-degradable products [158].

More recently, Nomadolo et al. investigated the biodegradation of PBAT/PLA and PBAT/PBS blend films under industrial (58 °C) and home (28 °C) composting conditions. The results showed that both blends degraded faster under industrial composting, with PBAT-PBS reaching 82% and PBAT-PLA reaching 90% mineralization in

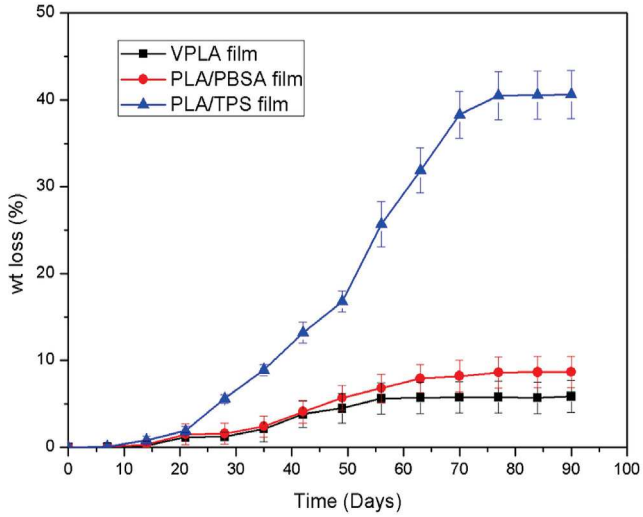

Fig. 23. Mass loss of PLA, PLA/PBSA film, and PLA/TPS film buried in soil. Duplicated with permission from Ref. [96].

120 days. Under home composting, PBAT-PBS and PBAT-PLA achieved 72% and 50% degradation in 200 days, respectively. FTIR, DSC, thermogravimetric analysis (TGA), X-ray diffraction (XRD), and SEM analyses confirmed degradation occurred through hydrolytic cleavage and microbial assimilation, with greater degradation of the PBAT component. The study demonstrated that industrial composting provides optimal conditions for the effective biodegradation of PBAT/PLA and PBAT/PBS blends.

In some other cases, blending can protect from microbial attack and slow the biodegradation rate. This can be very interesting to produce more durable bioplastic items that, under certain conditions, can still be biodegraded at the end of their life. It is the case of lignin, for example, which was proven to slow down the biodegradation rate of PHB in soil. Mousavioun et al. [159], for example, found that PHB films lost 45% of their mass when buried in soil for 12 months, but PHB films with just 10% lignin content lost only 12% mass over the same period. The lignin was proposed to inhibit microbial attack on the PHB. However, as Polman et al. pointed out in their review on the comparison of the aerobic biodegradation of biopolymers and the corresponding bioplastics [158], very little is known about the degradation mechanisms of lignin-based plastics, even though these findings may pave the way to tune the biodegradation rate of bioplastics in soil.

The situation is of course even more critical with blends where one parent polymer is not biodegradable, as with blends containing polyolefins [78,160,161] or toughening strategies for PLA and PHB involving non-degradable elastomers [156,79,72,82,162,163]. For example, Altayan et al. [78] blended wheat or corn starch with low-density polyethylene (LDPE) or linear low-density polyethylene (LLDPE), with and without a compatibilizer. As expected, the starch/PE blends showed increased biodegradability compared to pure PE. For the blends containing 15% starch, an α-amylase enzyme degradation test showed over 15% weight loss for all blends (16–18%) after 56 days, which the authors brought as evidence of biodegradation of both the starch and PE components. However, the authors did not carry out any tests to prove the effective biodegradation of PE (e.g., Fourier-transform infrared spectroscopy (FTIR), measurement of the molecular weight). Interestingly, the blends compatibilized with PE-g-MA showed a higher water uptake, which might be due to the carboxylic groups that formed during compatibilization, but it did not affect the biodegradation behavior. Tertyshnaya et al. [162] toughened PLA with 5 wt%, 10 wt %, and 15 wt% NR and tested the biodegradation under the action of soil microorganisms following a modified Sturm method. They found that for the 15% NR blend mass loss was 2.5% after 90 days, higher than that of neat PLA (1.2%), due to the microstructural rearrangement of PLA and the decreased crystallinity promoted by NR.

In any case, none of the found examples test the composting ability of the prepared PLA/rubber blends, as defined by several international standards. For example, ASTM D6400-19, which regulates products labeled as compostable in municipal or industrial aerobic facilities, other than imposing limits on residual, undegraded mass and on the negative influence on the final compost, states that each organic constituents present at levels between 1 and 10% shall be tested individually for compostability. Hence, in all these blends, NR or the other elastomers should *per se* demonstrate compostability and it is not enough to test the material as a whole.

When biodegradability or compositing ability is a property worth preserving, a good alternative can be using biodegradable elastomers. For example, Wang et al. [164] demonstrated that novel biodegradable elastomer particles (BEP) can be used to effectively toughen PLA while maintaining its biodegradability. Blending just 8 phr of BEP increased the elongation at break of PLA from 2.9% to 67.1% and its impact strength from 3.01 to 7.24 kJ/m^2. Unlike natural rubber, the biodegradable BEP did not hinder the biodegradation of the PLA composite. In fact, the PLA/BEP composites showed increased biodegradation rates compared to neat PLA in both soil and lipase solution experiments, as the BEP degraded faster than PLA, creating voids that accelerated PLA degradation.

7. Conclusions and future trends

This review has provided a comprehensive overview of the current strategies and recent advances in compatibilizing and tailoring the properties of biopolymer blends. Biopolymers, which are derived from renewable bio-based feedstocks and/or biodegradable, have emerged as a promising sustainable alternative to conventional plastics for packaging, medical, agricultural, and many other applications. However, limitations like brittleness, high cost, and restricted processability have hindered the widespread adoption of biopolymers. Blending offers an effective route to combine the strengths of different biopolymers and overcome these drawbacks. However, the inherent immiscibility between biopolymer pairs necessitates compatibilization to achieve optimal blend morphology, interfacial interactions, and synergistic properties.

Various physical and chemical compatibilization strategies have been explored for biopolymer blends, as detailed in this review. Non-reactive techniques utilizing block or graft copolymers with segments miscible in each phase represent a straightforward approach, though they are often limited in property enhancements. More impactful are reactive compatibilization methods, which form tailored copolymers in situ during melt blending at the interface between the phases. The reactive functional groups present on many biopolymers enable excellent opportunities for this reactive approach. Nanoparticle incorporation has also emerged as a highly versatile and multifunctional compatibilization route, which tailors phase morphology through selective nanofiller localization, which may also be tuned by a careful selection of the processing parameters.

Successful application of these strategies has been demonstrated for key biopolymer blend systems of industrial and academic interest. Compatibilized blends of PLA with biodegradable polyesters like PCL, PBAT, and PBS exhibit substantially improved toughness, ductility, and impact strength compared to the

intrinsically brittle PLA homopolymer. This expands PLA's utility beyond rigid items into flexible applications. Using plant polysaccharides like thermoplastic starch has also produced viable PLA and PHA blends with decreased cost and an acceptable balance of properties. Furthermore, properly compatibilized starch-polyester blends enable tuning of degradation rates as demanded for single-use plastics or long-lifetime applications. Nanoparticle incorporation additionally imparts functionality enhancements like gas barrier properties and flame retardancy.

However, opportunities remain for further advancing biopolymer blend performance and expanding real-world implementation through compatibilization strategies. Quantitatively correlating molecular interactions, miscibility, morphology development during processing, and final mechanical properties will enable more precise blend design and optimization. Understanding more deeply the chemical species and the new covalent bonds formed after reactive processing will enable full comprehension of the reactions taking place during the processing steps, allowing a finer tuning of the process parameters and the final microstructure and properties. Developing biopolymer-specific reactive chemistries and tailored nanoparticles offers potential for property improvements beyond what is achievable with conventional techniques. Compatibilization methods must also account for retaining full biodegradability and compostability, which are key advantages of biopolymer blends.

The growing production and diversity of biopolymers provide an extensive platform for creating next-generation blend materials through compatibilization. Blend systems with compatibilized morphologies and synergistic properties can fulfill specialized material demands across industries. Compatibilization is pivotal in enabling biopolymer blends to realize their immense potential as eco-friendly, high-performance, and cost-effective alternatives to traditional plastics. Continued research and development will facilitate the transition towards more sustainable and circular polymer materials and processes globally.

Author contributions

Andrea Dorigato: Writing – review & editing, Validation, Supervision, Funding acquisition. Giulia Fredi: Writing – review & editing, Writing – original draft, Methodology, Investigation, Conceptualization.

Declaration of competing interest

There is no conflict of interest.

Acknowledgments

This work received no external funding.

References

[1] Bioplastics: Facts and Figures, European Bioplastics - Nova Institute Report, 2022.
[2] R. Geyer, J.R. Jambeck, K.L. Law, Production, use, and fate of all plastics ever made, Sci. Adv. 3 (2017) 1700782.
[3] M. Bergmann, L. Gutow, M. Klages, Marine Anthropogenic Litter, SpringerOpen, 2015.
[4] K.D. Cox, G.A. Covernton, H.L. Davies, J.F. Dower, F. Juanes, S.E. Dudas, Human consumption of microplastics, Environ. Sci. Technol. 53 (12) (2019) 7068–7074.
[5] J.R. Jambeck, R. Geyer, C. Wilcox, T.R. Siegler, M. Perryman, A. Andrady, R. Narayan, K.L. Law, Plastic waste inputs from land into the ocean, Science 347 (6223) (2015) 768–771.
[6] G. Guidotti, M. Soccio, N. Lotti, M. Gazzano, V. Siracusa, A. Munari, Poly(propylene 2,5-thiophenedicarboxylate) vs. Poly(propylene 2,5-furandicarboxylate): two examples of high gas barrier bio-based polyesters, Polymers 10 (7) (2018).
[7] D. Garlotta, A literature review of poly(lactic acid), J. Polym. Environ. 9 (2) (2001) 63–84.
[8] W. Smitthipong, R. Chollakup, M. Nardin, Bio-Based Composites for High-Performance Materials: from Strategy to Industrial Application, CRC Press-Taylor & Francis Group, Boca Raton, FL, US, 2015.
[9] F.M. Lamberti, L.A. Román-Ramírez, J. Wood, Recycling of bioplastics: routes and benefits, J. Polym. Environ. 28 (10) (2020) 2551–2571.
[10] E. White, R. Bassilakis, S. Nogués, From the Plastics Present to a Sustainable Future: the Bioplastics Innovation Landscape, Players and Market Opportunities, Clarivate™, 2020.
[11] Y.-M. Corre, S. Bruzaud, J.-L. Audic, Y. Grohens, Morphology and functional properties of commercial polyhydroxyalkanoates: a comprehensive and comparative study, Polym. Test. 31 (2) (2012) 226–235.
[12] F. Valentini, A. Dorigato, D. Rigotti, A. Pegoretti, Polyhydroxyalkanoates/fibrillated nanocellulose composites for additive manufacturing, J. Polym. Environ. 27 (2019) 1333–1341.
[13] S.S. Ray, K. Okamoto, a.M. Okamoto, Structure-property relationship in biodegradable poly(butylene succinate)/layered silicate nanocomposites, Macromolecules 36 (2003) 2355–2367.
[14] A. Dorigato, D. Perin, A. Pegoretti, Effect of the temperature and of the drawing conditions on the fracture behaviour of thermoplastic starch films for packaging applications, J. Polym. Environ. 28 (2020) 3244–3255.
[15] A. Dorigato, G. Fredi, M. Negri, A. Pegoretti, Thermo-mechanical behaviour of novel wood laminae-thermoplastic starch biodegradable composites with thermal energy storage/release capability, Frontiers in Materials 6 (2019) 1–12.
[16] V. Siracusa, I. Blanco, Bio-polyethylene (Bio-PE), bio-polypropylene (Bio-PP) and bio-poly(ethylene terephthalate) (Bio-PET): recent developments in bio-based polymers analogous to petroleum-derived ones for packaging and engineering applications, Polymers 12 (8) (2020).
[17] M.H. Rahman, P.R. Bhoi, An overview of non-biodegradable bioplastics, J. Clean. Prod. 294 (2021) 126218.
[18] Plastics: the Facts, Plastics Europe - Report, 2022.
[19] B. Imre, L. Garcia, D. Puglia, F. Vilaplana, Reactive compatibilization of plant polysaccharides and biobased polymers: review on current strategies, expectations and reality, Carbohydr. Polym. 209 (2019) 20–37.
[20] B. Imre, B. Pukánszky, Compatibilization in bio-based and biodegradable polymer blends, Eur. Polym. J. 49 (6) (2013) 1215–1233.
[21] T.M. Letcher, Plastic Waste and Recycling: Environmental Impact, Societal Issues, Prevention, and Solutions, 2020.
[22] M. Niaounakis, Recycling of biopolymers – the patent perspective, Eur. Polym. J. 114 (2019) 464–475.
[23] G. Fredi, A. Dorigato, Recycling of bioplastic waste: a review, Advanced Industrial and Engineering Polymer Research 4 (2021) 159–177.
[24] J.B. Van Beilen, Y. Poirier, Production of renewable polymers from crop plants, Plant J. 54 (4) (2008) 684–701.
[25] A.J.R. Lasprilla, G.A.R. Martinez, B.H. Lunelli, A.L. Jardini, R.M. Filho, Poly-lactic acid synthesis for application in biomedical devices — a review, Biotechnol. Adv. 30 (1) (2012) 321–328.
[26] L. Avérous, Chapter 21 - polylactic acid: synthesis, properties and applications, in: M.N. Belgacem, A. Gandini (Eds.), Monomers, Polymers and Composites from Renewable Resources, Elsevier, 2008, pp. 433–450.
[27] J. Hu, J. Wang, M. Wang, Y. Ozaki, H. Sato, J. Zhang, Investigation of crystallization behavior of asymmetric PLLA/PDLA blend using Raman Imaging measurement, Polymer 172 (2019) 1–6.
[28] J. Kobayashi, T. Asahi, M. Ichiki, A. Oikawa, H. Suzuki, T. Watanabe, E. Fukada, Y. Shikinami, Structural and optical properties of poly lactic acids, J. Appl. Phys. 77 (7) (1995) 2957–2973.
[29] T. Maharana, B. Mohanty, Y.S. Negi, Melt–solid polycondensation of lactic acid and its biodegradability, Prog. Polym. Sci. 34 (2009) 99–124.
[30] M. Jamshidian, E.A. Tehrany, M. Imran, M. Jacquot, S. Desobry, Poly-lactic acid: production, applications, nanocomposites, and release studies, Compr. Rev. Food Sci. Food Saf. 9 (5) (2010) 552–571.
[31] X. Shi, J. Qin, L. Wang, L. Ren, F. Rong, D. Li, R. Wang, G. Zhang, Introduction of stereocomplex crystallites of PLA for the solid and microcellular poly(lactide)/poly(butylene adipate-co-terephthalate) blends, RSC Adv. 8 (22) (2018) 11850–11861.
[32] J. Cho, S. Baratian, J. Kim, F. Yeh, B.S. Hsiao, J. Runt, Crystallization and structure formation of poly(l-lactide-co-meso-lactide) random copolymers: a time-resolved wide- and small-angle X-ray scattering study, Polymer 44 (3) (2003) 711–717.
[33] N.-A.A.B. Taib, M.R. Rahman, D. Huda, K.K. Kuok, S. Hamdan, M.K.B. Bakri, M.R.M.B. Julaihi, A. Khan, A review on poly lactic acid (PLA) as a biodegradable polymer, Polym. Bull. 80 (2) (2023) 1179–1213.
[34] G. Fredi, E. Zonta, A. Dussin, D.N. Bikiaris, G.Z. Papageorgiou, L. Fambri, A. Dorigato, Toughening effect of 2,5-furandicaboxylate polyesters on polylactide-based renewable fibers, Molecules 28 (2023) 4811.
[35] D. Perin, G. Fredi, D. Rigotti, N. Lotti, A. Dorigato, Sustainable textile fibers made of bioderived polylactide/poly(pentamethylene 2,5-furanoate) blends, J. Appl. Polym. Sci. 139 (10) (2022) 51740.
[36] D. Perin, D. Rigotti, G. Fredi, G.Z. Papageorgiou, D.N. Bikiaris, A. Dorigato, Innovative bio-based poly(lactic acid)/poly(alkylene furanoate) fiber blends for sustainable textile applications, J. Polym. Environ. 29 (2021) 3948–3963.

[37] M. Tait, A. Pegoretti, A. Dorigato, K. Kalaitzidou, The effect of filler type and content and the manufacturing process on the performance of multifunctional carbon/poly-lactide composites, Carbon 49 (13) (2011) 4280–4290.
[38] A. Dorigato, M. Sebastiani, A. Pegoretti, L. Fambri, Effect of silica nanoparticles on the mechanical performances of poly(lactic acid), J. Polym. Environ. 20 (3) (2012) 713–725.
[39] L. Fambri, A. Dorigato, A. Pegoretti, Role of surface-treated silica nanoparticles on the thermo-mechanical behavior of poly(lactide), Appl. Sci. 10 (19) (2020) 6731.
[40] C. Fabris, D. Perin, G. Fredi, D. Rigotti, M. Bortolotti, A. Pegoretti, E. Xanthopoulou, D.N. Bikiaris, A. Dorigato, Improving the wet-spinning and drawing processes of poly(lactide)/poly(ethylene furanoate) and polylactide/poly(dodecamethylene furanoate) fiber blends, Polymers 14 (2022) 1910.
[41] G. Fredi, D. Rigotti, D.N. Bikiaris, A. Dorigato, Tuning thermo-mechanical properties of poly(lactic acid) films through blending with bioderived poly(alkylene furanoate)s with different alkyl chain length for sustainable packaging, Polymer 218 (2021) 123527.
[42] D. Rigotti, M. Soccio, A. Dorigato, M. Gazzano, V. Siracusa, G. Fredi, N. Lotti, Novel biobased polylactic acid/poly(pentamethylene 2,5-furanoate) blends for sustainable food packaging, ACS Sustain. Chem. Eng. 9 (41) (2021) 13742–13750.
[43] M. Niaounakis, Chapter 1 - introduction, in: M. Niaounakis (Ed.), Biopolymers: Processing and Products, William Andrew Publishing, Oxford, 2015, pp. 1–77.
[44] S.K. Bhatia, S.V. Otari, J.M. Jeon, R. Gurav, Y.K. Choi, R.K. Bhatia, A. Pugazhendhi, V. Kumar, J.R. Banu, J.J. Yoon, K.Y. Choi, Y.H. Yang, Biowaste-to-bioplastic (polyhydroxyalkanoates): conversion technologies, strategies, challenges, and perspective, Bioresour. Technol. 326 (2021).
[45] Z.A. Raza, S. Abid, I.M. Banat, Polyhydroxyalkanoates: characteristics, production, recent developments and applications, Int. Biodeterior. Biodegrad. 126 (2018) 45–56.
[46] R. Amache, A. Sukan, M. Safari, I. Roy, T. Keshavarz, Advances in PHAs production, Chemical Engineering Transactions 32 (2013) 931–936.
[47] A. Anjum, M. Zuber, K.M. Zia, A. Noreen, M.N. Anjum, S. Tabasum, Microbial production of polyhydroxyalkanoates (PHAs) and its copolymers: a review of recent advancements, Int. J. Biol. Macromol. 89 (2016) 161–174.
[48] S.Y. Choi, M.N. Rhie, H.T. Kim, J.C. Joo, I.J. Cho, J. Son, S.Y. Jo, Y.J. Sohn, K.A. Baritugo, J. Pyo, Y. Lee, S.Y. Lee, S.J. Park, Metabolic engineering for the synthesis of polyesters: a 100-year journey from polyhydroxyalkanoates to non-natural microbial polyesters, Metab. Eng. 58 (2020) 47–81.
[49] V.C. Kalia, S.K.S. Patel, R. Shanmugam, J.K. Lee, Polyhydroxyalkanoates, Trends and advances toward biotechnological applications, Bioresour. Technol. 326 (2021).
[50] L. Lorini, A. Martinelli, G. Capuani, N. Frison, M. Reis, B.S. Ferreira, M. Villano, M. Majone, F. Valentino, Characterization of polyhydroxyalkanoates produced at pilot scale from different organic wastes, Front. Bioeng. Biotechnol. 9 (2021).
[51] J.B. Silva, J.R. Pereira, B.C. Marreiros, M.A.M. Reis, F. Freitas, Microbial production of medium-chain length polyhydroxyalkanoates, Process Biochem. 102 (2021) 393–407.
[52] European Bioplastics Association, Bioplastics: Facts and Figure, 2019. Berlin, Germany.
[53] M. Niaounakis, Biopolymers Reuse, Recycling, and Disposal, Elsevier, Oxford, UK, 2013.
[54] A. Shafqat, A. Tahir, A. Mahmood, A.B. Tabinda, A. Yasar, A. Pugazhendhi, A review on environmental significance carbon foot prints of starch based bio-plastic: a substitute of conventional plastics, Biocatal. Agric. Biotechnol. 27 (2020).
[55] A.H.M. Zain, M.K. Ab Wahab, H. Ismail, Biodegradation behaviour of thermoplastic starch: the roles of carboxylic acids on cassava starch, J. Polym. Environ. 26 (2) (2017) 691–700.
[56] H. Meriem, C. Messaoud, H. Badra, B. Anissa, Biodegradation of plastic film based on starch, Biointerface Research in Applied Chemistry 6 (5) (2016) 1517–1519.
[57] M.K. Marichelvam, M. Jawaid, M. Asim, Corn and rice starch-based bioplastics as alternative packaging materials, Fibers 7 (4) (2019).
[58] T. Ma, A Study on Moulding Technology of Starch-Based Totally-Biodegradable Plastic Products, Advances in Environmental Technologies, 2013, pp. 622–628. Pts 1-6.
[59] E.J. Eterigho, T.S. Farrow, E.E. Silver, G.O. Daniel, Study of the physical properties and biodegradability of potato-starch based plastics, world congress on engineering and computer science, Wcecs Ii2017 (2017) 637–641.
[60] N. Meite, L.K. Konan, D. Bamba, B.I.H. Goure-Doubi, S. Oyetola, Thermo-mechanical properties of plastic films based on cassava starch reinforced with kaolin and metakaolin, Recent Advances in Environmental Science from the Euro-Mediterranean and Surrounding Regions I and Ii (2018) 123–124.
[61] E.M. Nagy, M. Todica, C. Cota, V.C. Pop, N. Cioica, O. Cozar, Water degradation effect on some starch-based plastics, in: Aktualni Zadaci Mehanizacije Poljoprivrede: Actual Tasks on Agricultural Engineering, 2015, pp. 755–762.
[62] L.A. Utracki, C.A. Wilkie, Polymer Blends Handbook, Springer Netherlands, 2014.
[63] A. Dorigato, A. Pegoretti, L. Fambri, C. Lonardi, M. Slouf, J. Kolarik, Linear low density polyethylene - cycloolefin copolymer blends, Express Polym. Lett. 5 (1) (2011) 23–37.
[64] Z. Horak, I. Fortelny, J. Kolarik, D. Hlavata, A. Sikora, Polymer Blends, Encyclopedia of Polymer Scince and Technology, John Wiley & Sons Inc., 2005.
[65] F.P. La Mantia, M. Morreale, L. Botta, M.C. Mistretta, M. Ceraulo, R. Scaffaro, Degradation of polymer blends: a brief review, Polym. Degrad. Stabil. 145 (2017) 79–92.
[66] L.A. Utracki, Polymer Blends Handbook, Kluwer academic publishers, 2002.
[67] B.D. Gesner, Encyclopedia of Polymer Science and Technology, vol. 10, Interscience, New York, 1969.
[68] A. Surendren, A.K. Mohanty, Q. Liuc, M. Misra, A review of biodegradable thermoplastic starches, their blends and composites: recent developments and opportunities for single-use plastic packaging alternatives, Green Chem. 24 (2022) 8606.
[69] V. Goel, P. Luthra, G.S. Kapur, S.S.V. Ramakumar, Biodegradable/Bio-plastics: myths and realities, J. Polym. Environ. 29 (10) (2021) 3079–3104.
[70] E. Leroy, P. Jacquet, G. Coativy, A.L. Reguerre, D. Lourdin, Compatibilization of starch-zein melt processed blends by an ionic liquid used as plasticizer, Carbohydr. Polym. 89 (3) (2012) 955–963.
[71] M.F.C. de Andrade, H.C. Loureiro, C. Sarantopoulos, A.R. Morales, Blends of poly (butylene adipate-Co-terephthalate) and thermoplastic whey protein isolate: a compatibilization study, J. Polym. Environ. 29 (10) (2021) 3288–3301.
[72] N.A. Rosli, I. Ahmad, F.H. Anuar, I. Abdullah, Effectiveness of cellulosic Agave angustifolia fibres on the performance of compatibilised poly(lactic acid)-natural rubber blends, Cellulose 26 (5) (2019) 3205–3218.
[73] Y. Ding, B. Lu, P. Wang, G. Wang, J. Ji, PLA-PBAT-PLA tri-block copolymers: effective compatibilizers for promotion of the mechanical and rheological properties of PLA/PBAT blends, Polym. Degrad. Stabil. 147 (2018) 41–48.
[74] L. Shang, S. Qu, Y. Deng, Y. Gao, G. Yue, S. He, Z. Wang, Z. Wang, F. Tan, Simple furan-based polymers with the self-healing function enable efficient eco-friendly organic solar cells with high stability, J. Mater. Chem. C 10 (2) (2022) 506–516.
[75] G. Conde, J.R.G. de Carvalho, P.D. Dias, H.G. Moranza, G.L. Montanhim, J.D. Ribeiro, M.A. Chinelatto, P.C. Moraes, S.R. Taboga, P.H.L. Bertolo, M.I.G. Funnicelli, D.G. Pinheiro, G.D. Ferraz, In vivo biocompatibility and biodegradability of poly(lactic acid)/poly(epsilon-caprolactone) blend compatibilized with poly(epsilon-caprolactone-b-tetrahydrofuran) in Wistar rats, Biomedical Physics & Engineering Express 7 (3) (2021) 035005.
[76] N. Nomadolo, O.E. Dada, A. Swanepoel, T. Mokhena, S. Muniyasamy, A comparative study on the aerobic biodegradation of the biopolymer blends of poly(butylene succinate), poly(butylene adipate terephthalate) and poly(lactic acid), Polymers 14 (2022) 1894.
[77] W. He, L. Ye, P. Coates, F. Caton-Rose, X. Zhao, Reactive processing of poly(lactic acid)/poly(ethylene octene) blend film with tailored interfacial intermolecular entanglement and toughening mechanism, J. Mater. Sci. Technol. 98 (2022) 186–196.
[78] M.M. Altayan, T. Al Darouich, Toward reducing the food packaging waste impact: a study on the effect of Starch type and PE type in thermoplastic starch-polyethylene blends, Chem. Pap. 76 (4) (2022) 2447–2457.
[79] C. Ozbay, O.Y. Gumus, Enhanced strength and toughness of polylactic acid by blending with modified natural rubber having acetate pendant group, J. Elastomers Plast. 55 (5) (2023) 653–676.
[80] A.S. Walallavita, C.J.R. Verbeek, M.C. Lay, Biopolymer foams from Novatein thermoplastic protein and poly(lactic acid), J. Appl. Polym. Sci. 134 (48) (2017) 45561.
[81] K. Prasanna, R.R.N. Sailaja, Blends of LDPE/chitosan using epoxy-functionalized LDPE as compatibilizer, J. Appl. Polym. Sci. 124 (4) (2012) 3264–3275.
[82] L. Musa, N. Krishna Kumar, S.Z. Abd Rahim, M.S. Mohamad Rasidi, A.E. Watson Rennie, R. Rahman, A. Yousefi Kanani, A.A. Azmi, A review on the potential of polylactic acid based thermoplastic elastomer as filament material for fused deposition modelling, J. Mater. Res. Technol. 20 (2022) 2841–2858.
[83] C.Y. Wu, W.B. Lui, J. Peng, Optimization of extrusion variables and maleic anhydride content on biopolymer blends based on poly(hydroxybutyrate-co-hydroxyvalerate)/poly(vinyl acetate) with tapioca starch, Polymers 10 (8) (2018) 827.
[84] X.-Z. Mo, F.-X. Wei, D.-F. Tan, J.-Y. Pang, C.-B. Lan, The compatibilization of PLA-g-TPU graft copolymer on polylactide/thermoplastic polyurethane blends, J. Polym. Res. 27 (2) (2020) 33.
[85] J.Y. Gong, Z. Qiang, J. Ren, In situ grafting approach for preparing PLA/PHBV degradable blends with improved mechanical properties, Polym. Bull. 79 (11) (2022) 9543–9562.
[86] B. Wang, X. Ye, B.W. Wang, X.P. Li, S.L. Xiao, H.S. Liu, Reactive graphene as highly efficient compatibilizer for cocontinuous poly (lactic acid)/poly(epsilon-caprolactone) blends toward robust biodegradable nanocomposites, Compos. Sci. Technol. 221 (2022) 109326.
[87] W. Phetwarotai, M. Zawong, N. Phusunti, D. Aht-Ong, Toughening and thermal characteristics of plasticized polylactide and poly(butylene adipate-co-terephthalate) blend films: influence of compatibilization, Int. J. Biol. Macromol. 183 (2021) 346–357.
[88] Y. Zhou, J. Wang, S.Y. Cai, Z.G. Wang, N.W. Zhang, J. Ren, Effect of POE-g-GMA on mechanical, rheological and thermal properties of poly(lactic acid)/poly(propylene carbonate) blends, Polym. Bull. 75 (12) (2018) 5437–5454.
[89] L. Quiles-Carrillo, N. Montanes, J.M. Lagaron, R. Balart, S. Torres-Giner, In situ compatibilization of biopolymer ternary blends by reactive extrusion with

low-functionality epoxy-based styrene-acrylic oligomer, J. Polym. Environ. 27 (1) (2019) 84–96.
[90] B.A. Calderon, M.S. McCaughey, C.W. Thompson, V.L. Barinelli, M.J. Sobkowicz, Evaluating the influence of specific mechanical energy on biopolymer blends prepared via high-speed reactive extrusion, ACS Appl. Polym. Mater. 1 (6) (2019) 1410–1419.
[91] L. Quiles-Carrillo, N. Montanes, A. Jorda-Vilaplana, R. Balart, S. Torres-Giner, A comparative study on the effect of different reactive compatibilizers on injection-molded pieces of bio-based high-density polyethylene/polylactide blends, J. Appl. Polym. Sci. 136 (16) (2019) 47396.
[92] Y. Fourati, Q. Tarres, P. Mutje, S. Boufi, PBAT/thermoplastic starch blends: effect of compatibilizers on the rheological, mechanical and morphological properties, Carbohydr. Polym. 199 (2018) 51–57.
[93] N. Wu, H. Zhang, Mechanical properties and phase morphology of super-tough PLA/PBAT/EMA-GMA multicomponent blends, Mater. Lett. 192 (2017) 17–20.
[94] P. Ma, X. Cai, Y. Zhang, S. Wang, W. Dong, M. Chen, P.J. Lemstra, In-situ compatibilization of poly(lactic acid) and poly(butylene adipate-co-terephthalate) blends by using dicumyl peroxide as a free-radical initiator, Polym. Degrad. Stabil. 102 (2014) 145–151.
[95] C. Kaynak, Y. Meyva, Use of maleic anhydride compatibilization to improve toughness and other properties of polylactide blended with thermoplastic elastomers, Polym. Adv. Technol. 25 (12) (2014) 1622–1632.
[96] B. Palai, S. Mohanty, S.K. Nayak, A comparison on biodegradation behaviour of polylactic acid (PLA) based blown films by incorporating thermoplasticized starch (TPS) and poly (butylene succinate-co-adipate) (PBSA) biopolymer in soil, J. Polym. Environ. 29 (9) (2021) 2772–2788.
[97] J. Urquijo, N. Aranburu, S. Dagréou, G. Guerrica-Echevarría, J.I. Eguiazábal, CNT-induced morphology and its effect on properties in PLA/PBAT-based nanocomposites, Eur. Polym. J. 93 (2017) 545–555.
[98] Y. Ahmadzadeh, A. Babaei, A. Goudarzi, Assessment of localization and degradation of ZnO nano-particles in the PLA/PCL biocompatible blend through a comprehensive rheological characterization, Polym. Degrad. Stabil. 158 (2018) 136–147.
[99] V. Sessini, I. Navarro-Baena, M.P. Arrieta, F. Dominici, D. López, L. Torre, J.M. Kenny, P. Dubois, J.-M. Raquez, L. Peponi, Effect of the addition of polyester-grafted-cellulose nanocrystals on the shape memory properties of biodegradable PLA/PCL nanocomposites, Polym. Degrad. Stabil. 152 (2018) 126–138.
[100] I. Zembouai, M. Kaci, L. Zaidi, S. Bruzaud, Combined effects of Sepiolite and Cloisite 30B on morphology and properties of poly(3-hydroxybutyrate-co-3-hydroxyvalerate)/polylactide blends, Polym. Degrad. Stabil. 153 (2018) 47–52.
[101] J. Yang, X. Qi, N. Zhang, T. Huang, Y. Wang, Carbon nanotubes toughened immiscible polymer blends, Compos. Commun. 7 (2018) 51–64.
[102] B. Zhu, T. Bai, P. Wang, Y. Wang, C. Liu, C. Shen, Selective dispersion of carbon nanotubes and nanoclay in biodegradable poly(epsilon-caprolactone)/poly(lactic acid) blends with improved toughness, strength and thermal stability, Int. J. Biol. Macromol. 153 (2020) 1272–1280.
[103] W.N. Kim, C.M. Burns, Blends of polycarbonate and poly(-methylmethacrylate) and the determination of the polymer-polymer interaction parameter of the two polymers, Macromolecules 20 (1987) 1876–1882.
[104] T. Nishi, T.T. Wang, Melting point depression and kinetic effects of cooling on crystallization in poly(viny1idene fluoride)-poly (methyl methacrylate) mixtures, Macromolecules 8 (6) (1975) 909–915.
[105] Y. Meng, X. Zhang, Nanostructure Formation in thermoset/block copolymer and thermoset/hyperbranched polymer blends, in: S. Thomas, R. Shanks, S. Chandrasekharakurup (Eds.), Nanostructured Polymer Blends, William Andrew, 2014, pp. 161–194.
[106] Y. Lan, M.G. Corradini, X. Liu, T.E. May, F. Borondics, R.G. Weiss, M.A. Rogers, Comparing and correlating solubility parameters governing the self-assembly of molecular gels using 1,3:2,4-dibenzylidene sorbitol as the gelator, Langmuir 30 (47) (2014) 14128–14142.
[107] M.M. Coleman, P.C. Painter, J.F. Graf, Specific Interactions and the Miscibility of Polymer Blends, Technomic Publishing Company, Inc., Lancaster, Pennsylvania, 1991.
[108] N. Tuancharoensri, G.M. Ross, A. Kongprayoon, S. Mahasaranon, S. Pratumshat, J. Viyoch, N. Petrot, W. Ruanthong, W. Punyodom, P.D. Topham, B.J. Tighe, S. Ross, In situ compatibilized blends of PLA/PCL/CAB melt-blown films with high elongation: investigation of miscibility, morphology, crystallinity and modelling, Polymers 15 (2) (2023) 303.
[109] B. Oner, T. Gokkurt, A. Aytac, Studies on compatibilization of recycled polyethylene/thermoplastic starch blends by using different compatibilizer, Open Chem. 17 (1) (2019) 557–563.
[110] V. Mittal, T. Akhtar, G. Luckachan, N. Matsko, PLA, TPS and PCL binary and ternary blends: structural characterization and time-dependent morphological changes, Colloid Polym. Sci. 293 (2) (2015) 573–585.
[111] N.S. Yatigala, D.S. Bajwa, S.G. Bajwa, Compatibilization improves physico-mechanical properties of biodegradable biobased polymer composites, Compos. Appl. Sci. Manuf. 107 (2018) 315–325.
[112] J. Favero, S. Belhabib, S. Guessasma, P. Decaen, A.L. Reguerre, D. Lourdin, E. Leroy, On the representative elementary size concept to evaluate the compatibilisation of a plasticised biopolymer blend, Carbohydr. Polym. 172 (2017) 120–129.
[113] M. Mehrabi Mazidi, H. Sharifi, M.K. Razavi Aghjeh, L. Zare, H.A. Khonakdar, U. Reuter, Super-tough PLA-based blends with excellent stiffness and greatly improved thermal resistance via interphase engineering, ACS Appl. Mater. Interfaces 15 (18) (2023) 22445–22470.
[114] A. Avci, A.A. Eker, M.S. Bodur, Influence of compatibilization and internal lubricant on the mechanical and thermo-mechanical properties of PLA/TPU compound, Polymer-Korea 46 (5) (2022) 671–683.
[115] X. Wang, S. Peng, H. Chen, X. Yu, X. Zhao, Mechanical properties, rheological behaviors, and phase morphologies of high-toughness PLA/PBAT blends by in-situ reactive compatibilization, Compos. B Eng. 173 (2019) 107028.
[116] V.H. Sangeetha, H. Deka, T.O. Varghese, S.K. Nayak, State of the art and future prospectives of poly(lactic acid) based blends and composites, Polym. Compos. 39 (1) (2018) 81–101.
[117] B.P. Chang, A.K. Mohanty, M. Misra, Tuning the compatibility to achieve toughened biobased poly(lactic acid)/poly(butylene terephthalate) blends, RSC Adv. 8 (49) (2018) 27709–27724.
[118] G. Fredi, M.K. Jafari, A. Dorigato, D.N. Bikiaris, A. Pegoretti, Improving the thermomechanical properties of poly(lactic acid) via reduced graphene oxide and bioderived poly(decamethylene 2,5-furandicarboxylate), Materials 15 (4) (2022) 1316.
[119] G. Fredi, M.K. Jafari, A. Dorigato, D.N. Bikiaris, R. Checchetto, M. Favaro, R.S. Brusa, A. Pegoretti, Multifunctionality of reduced graphene oxide in bioderived polylactide/poly(dodecylene furanoate) nanocomposite films, Molecules 26 (10) (2021) 2398.
[120] F. Sarasini, F. Luzi, F. Dominici, G. Maffei, A. Iannone, A. Zuorro, R. Lavecchia, L. Torre, A. Carbonell-Verdu, R. Balart, D. Puglia, Effect of different compatibilizers on sustainable composites based on a PHBV/PBAT matrix filled with coffee silverskin, Polymers 10 (11) (2018) 1256.
[121] P. Feijoo, K. Samaniego-Aguilar, E. Sanchez-Safont, S. Torres-Giner, J.M. Lagaron, J. Gamez-Perez, L. Cabedo, Development and characterization of fully renewable and biodegradable polyhydroxyalkanoate blends with improved thermoformability, Polymers 14 (13) (2022) 2527.
[122] J.L. Barbosa, G.B. Perin, M.I. Felisberti, Plasticization of poly(3-hydroxybutyrate-co-3-hydroxyvalerate) with an oligomeric polyester: miscibility and effect of the microstructure and plasticizer distribution on thermal and mechanical properties, ACS Omega 6 (4) (2021) 3278–3290.
[123] A.M. El-Hadi, The effect of additives interaction on the miscibility and crystal structure of two immiscible biodegradable polymers, Polímeros - Ciência Tecnol. 24 (1) (2014) 9–16.
[124] S. Wu, Polymer Interface and Adhesion, Taylor & Francis Group, Boca Raton, FL, USA, 1982.
[125] M. Salzano de Luna, G. Filippone, Effects of nanoparticles on the morphology of immiscible polymer blends – challenges and opportunities, Eur. Polym. J. 79 (2016) 198–218.
[126] A. Ryan, Designer polymer blends, Nat. Mater. 1 (2002) 8–10.
[127] S. Datta, D.J. Lohse, Polymeric Compatibilizers, Carl Hanser Verlag, Munich, 1996.
[128] I. Fortelny, J. Juza, The effects of copolymer compatibilizers on the phase structure evolution in polymer blends-A review, Materials 14 (24) (2021) 7786.
[129] Y. Ding, W. Feng, D. Huang, B. Lu, P. Wang, G. Wang, J. Ji, Compatibilization of immiscible PLA-based biodegradable polymer blends using amphiphilic di-block copolymers, Eur. Polym. J. 118 (2019) 45–52.
[130] R. Al-Itry, K. Lamnawar, A. Maazouz, Reactive extrusion of PLA, PBAT with a multi-functional epoxide: physico-chemical and rheological properties, Eur. Polym. J. 58 (2014) 90–102.
[131] C. Aversa, M. Barletta, G. Cappiello, A. Gisario, Compatibilization strategies and analysis of morphological features of poly (butylene adipate-co-terephthalate) (PBAT)/poly(lactic acid) PLA blends: a state-of-art review, Eur. Polym. J. 173 (2022) 111304.
[132] L.A. Utracki, Commercial Polymer Blends, Springer, US, 1998.
[133] A. Pegoretti, A. Dorigato, Polymer Composites: Reinforcing Fillers, Encyclopedia of Polymer Science and Technology, 2019, pp. 1–72.
[134] V. Shifrin, Y.S. Lipatov, A.Y. Nesterov, The introduction of a filler and consequent increase in the thermodynamic compatibility of binary polyblends, Polym. Sci. 27 (2) (1985) 412–417.
[135] P.M. Ajayan, L.S. Schadler, P.V. Braun, Nanocomposite Science and Technology, Wiley-VCH Verlag GmbH & Co. KGaA, Weinheim (Germany), 2003.
[136] M.J. Mochane, J.S. Sefadi, T.S. Motsoeneng, T.E. Mokoena, T.G. Mofokeng, T.C. Mokhena, The effect of filler localization on the properties of biopolymer blends, recent advances: a review, Polym. Compos. 41 (7) (2020) 2958–2979.
[137] A.R. Ajitha, L.P. Mathew, S. Thomas, Compatibilization of Polymer Blends by Micro and Nanofillers, Compatibilization of Polymer Blends: Micro and Nano Scale Phase Morphologies, Interphase Characterization, and Properties, 2019, pp. 179–203.
[138] S. Das, S.K. Samal, S. Mohanty, S.K. Nayak, Crystallization of polymer blend nanocomposites, Crystallization in Multiphase Polymer Systems (2018) 313–339.
[139] A. Nesterov, Y. Lipatov, Compatibilizing effect of a filler in binary polymer mixtures, Polymer 40 (5) (1999) 1347–1349.
[140] V.V. Ginzburg, Influence of nanoparticles on miscibility of polymer blends. A simple theory, Macromolecules 38 (6) (2005) 2362–2367.
[141] S. George, K. Ramamurthy, J. Anand, G. Groeninckx, K. Varughese, S. Thomas, Rheological behaviour of thermoplastic elastomers from polypropylene/

acrylonitrileebutadiene rubber blends: effect of blend ratio, reactive compatibilization and dynamic vulcanization, Polymer 40 (15) (1999) 4325–4344.
[142] D. Shahdan, N.A. Rosli, R.S. Chen, S. Ahmad, A feasible compatibilization processing technique for improving the mechanical and thermal performance of rubbery biopolymer/graphene nanocomposites, Polymers 14 (22) (2022) 5009.
[143] J. Chen, X.C. Du, W.B. Zhang, J.H. Yang, N. Zhang, T. Huang, Y. Wang, Synergistic effect of carbon nanotubes and carbon black on electrical conductivity of PA6/ABS blend, Compos. Sci. Technol. 81 (2013) 1–8.
[144] J. Chen, Y.Y. Shi, J.H. Yang, N. Zhang, T. Huang, C. Chen, Y. Wang, Z.W. Zhou, A simple strategy to achieve very low percolation threshold via the selective distribution of carbon nanotubes at the interface of polymer blends, J. Mater. Chem. 22 (42) (2012) 22398–22404.
[145] D. Wu, Y. Sun, D. Lin, W. Zhou, M. Zhang, L. Yuan, Selective localization behavior of carbon nanotubes: effect on transesterification of immiscible polyester blends, Macromol. Chem. Phys. 212 (15) (2011) 1700–1709.
[146] Y. Son, Measurement of interface free energy in polypropylene/ethyleneepropylene rubber blends, J. Adhes. 9 (12) (2015) 909–919.
[147] S. Nuriel, L. Liu, A. Barber, H. Wagner, Direct measurement of multiwall nanotube surface tension, Chem. Phys. Lett. 404 (4) (2005) 263–266.
[148] S.T. Nair, P.P. Vijayan, P. Xavier, S. Bose, S.C. George, S. Thomas, Selective localisation of multi walled carbon nanotubes in polypropylene/natural rubber blends to reduce the percolation threshold, Compos. Sci. Technol. 116 (2015) 9–17.
[149] M.H. Al-Saleh, Carbon nanotube-filled polypropylene/polyethylene blends: compatibilization and electrical properties, Polym. Bull. 73 (4) (2016) 975–987.
[150] M. Nofar, M.C. Heuzey, P.J. Carreau, M.R. Kamal, Effects of nanoclay and its localization on the morphology stabilization of PLA/PBAT blends under shear flow, Polymer 98 (2016) 353–364.
[151] C. Koning, M.V. Duin, C. Pagnoulle, R. Jerome, Strategies for compatibilization of polymer blends, Prog. Polym. Sci. 23 (1998) 707–757.
[152] R. Al-Itry, K. Lamnawar, A. Maazouz, Rheological, morphological, and interfacial properties of compatibilized PLA/PBAT blends, Rheologica Acta 53 (7) (2014) 501–517.
[153] G. Fredi, A. Dorigato, A. Dussin, E. Xanthopoulou, D.N. Bikiaris, L. Botta, V. Fiore, A. Pegoretti, Compatibilization of polylactide/poly(ethylene furanoate) (PLA/PEF) blends for sustainable and bioderived packaging, Molecules 27 (2022) 6371.
[154] E. Fekete, B. Pukanszky, Z. Peredy, Mutual correlations between parameters characterizing the miscibility, structure and mechanical properties of polymer blends, Die Angewandte Makromolekulare Chemie 199 (1992) 87–101.
[155] M. Ramos, F. Dominici, F. Luzi, A. Jimenez, M.C. Garrigos, L. Torre, D. Puglia, Effect of almond shell waste on physicochemical properties of polyester-based biocomposites, Polymers 12 (4) (2020) 835.
[156] K. Suthapakti, R. Molloy, W. Punyodom, K. Nalampang, T. Leejarkpai, P.D. Topham, B.J. Tighe, Biodegradable compatibilized poly(l-lactide)/thermoplastic polyurethane blends: design, preparation and property testing, J. Polym. Environ. 26 (5) (2017) 1818–1830.
[157] C. Hou, X. Sun, Z. Ren, H. Li, S. Yan, Polymorphism and enzymatic degradation of poly(1,4-butylene adipate) and its binary blends with atactic poly(3-hydroxybutyrate) and poly(vinyl phenol), Ind. Eng. Chem. Res. 56 (48) (2017) 14263–14269.
[158] E.M.N. Polman, G.M. Gruter, J.R. Parsons, A. Tietema, Comparison of the aerobic biodegradation of biopolymers and the corresponding bioplastics: a review, Sci. Total Environ. 753 (2021) 141953.
[159] P. Mousavioun, G.A. George, W.O.S. Doherty, Environmental degradation of lignin/poly(hydroxybutyrate) blends, Polym. Degrad. Stabil. 97 (7) (2012) 1114–1122.
[160] M.N.F. Norrrahim, H. Ariffin, M.A. Hassan, N.A. Ibrahim, H. Nishida, Performance evaluation and chemical recyclability of a polyethylene/poly(3-hydroxybutyrate-co-3-hydroxyvalerate) blend for sustainable packaging, RSC Adv. 3 (46) (2013) 24378.
[161] A. Abioye, C. Obuekwe, O. Fasanmi, O. Oluwadare, O. Abioye, S. Afolalu, S. Akinlabi, C. Bolu, Investigation of biodegradation speed and biodegradability of polyethylene and manihot esculenta starch blends, Journal of Ecological Engineering 20 (2) (2019) 65–72.
[162] Y.V. Tertyshnaya, M.V. Podzorova, A.V. Khramkova, V.A. Ovchinnikov, A.V. Krivandin, Structural rearrangements of polylactide/natural rubber composites during hydro- and biotic degradation, Polymers 15 (2023) 1930.
[163] M.R. Ketabchi, S. Masoudi Soltani, A. Chan, Synthesis of a new biocomposite for fertiliser coating: assessment of biodegradability and thermal stability, Environ. Sci. Pollut. Res. Int. 30 (41) (2023) 93722–93730.
[164] Q. Wang, Y. Li, X. Zhou, T. Wang, L. Qiu, Y. Gu, J. Chang, Toughened poly(lactic acid)/BEP composites with good biodegradability and cytocompatibility, Polymers 11 (9) (2019) 1413.